EUROPEAN ORGANIZATION FOR PARTICLE PHYSICS

LEPEWWG/95-02
ALEPH 95-093 PHYSIC 95-086
DELPHI 95-137 PHYS 562
L3 Note 1814
OPAL Technical Note TN312
1 August 1995

A Combination of Preliminary LEP Electroweak Results for the 1995 Summer Conferences

LEP Electroweak Working Group*

Internal Note

Prepared from Contributions of the LEP Experiments to the 1995 International Europhysics Conference on High Energy Physics, 27/7 to 2/8/1995, Brussels, Belgium and the 17th International Symposium on Lepton-Photon Interactions, 10-15/8 1995, Beijing, China.

Abstract

This note presents a combination of published and preliminary electroweak results from the four LEP collaborations which were prepared for the 1995 summer conferences. Averages of electroweak LEP results from the measurement of hadronic and leptonic cross sections, the leptonic forward-backward asymmetries, the τ polarization asymmetries, the $b\overline{b}$ and $c\overline{c}$ partial widths and forward-backward asymmetries and the $q\overline{q}$ charge asymmetry are presented. The LEP results are then compared to precise electroweak tests from other experiments. The parameters of the Standard Model are evaluated, first using the combined LEP electroweak measurements, and then using the full set of precise electroweak results. For the first time the LEP and SLD heavy flavour results are combined in a consistent manner with the help of members of the SLD collaboration.

*The present members of the LEP Electroweak Working Group are: P. Antilogus, T. Behnke A. Blondel, I. Brock, J. Busenitz, D. Charlton, R. Clare, P. Clarke, S. Ganguli, M. Grünewald, A. Gurtu, R.W.L. Jones, A. Kounine, M. Mannelli, M. Martinez, K. Mönig, G. Myatt, A. Olshevsky, A. Passeri, Ch. Paus, M. Pepe-Altarelli, P. Perret, B. Pietrzyk, P. Renton, D. Reid, M. Roney, D. Schaile, D. Schlatter, T.J. Smith, R. Tenchini, F. Teubert, P. Wells.

1 Introduction

In a recent note [1] the four LEP experiments have presented parameters of the Z resonance derived from published and preliminary results based on data recorded until the end of 1993. Most of the preliminary results were contributions to the 27th International Conference on High Energy Physics, Glasgow, Scotland, 20-27 July 1994.

Since then several preliminary analyses have been completed and published. Also the calibration of the LEP energy scale for the high statistics scan of the Z resonance in 1993 has been finalized [2] resulting in improved uncertainties due to LEP energies on the Z mass, m_{Z}, and total width, Γ_{Z}.

Furthermore several new preliminary results from the 1994 running period have become available. In 1994 the LEP experiments approximately doubled their event statistics. Important progress has also been achieved for the theoretical error associated to the luminosity determination [3]. It is expected that an even better theoretical precision will finally be obtained. The interpretation of electroweak precision data requires a precise knowledge of the fine structure constant evaluated at the Z pole, $\alpha(m_{\mathrm{Z}}^2)$, for which several reevaluations have been performed recently [4–7]. Last but not least, the CDF and DØ collaborations have published their discovery of the top quark [8,9].

The data consist of the hadronic and leptonic cross sections, the leptonic forward-backward asymmetries, the τ polarization asymmetries, the $\mathrm{b\overline{b}}$ and $\mathrm{c\overline{c}}$ partial widths and forward-backward asymmetries and the $\mathrm{q\overline{q}}$ charge asymmetry. Many technical aspects of their combination have already been described in [1] and references therein.

This note is organised in the following manner. In Section 2 the results on the Z line shape and leptonic forward-backward asymmetries are presented, and Section 3 contains the measurements of the τ polarization. Section 4 describes the parameters associated with heavy flavour analyses, Section 5 new results for the inclusive hadronic charge asymmetry. In Sections 6.1 and 6.2 several LEP electroweak measurements are combined to determine the effective neutral current coupling constants and to give a value of the effective electroweak mixing angle. We also quote results for these parameters when the left-right polarization asymmetry SLD [10,11] is included. The number of light neutrinos is determined in Section 6.3. In Section 6.4 first the LEP data and then also data from SLD [10–16], from neutrino interactions [17–19] and from measurements of the mass of the W boson [20–23] and the top quark [8,9] are used to constrain the parameters of the Standard Model.

2 Z Lineshape and Lepton Forward-Backward Asymmetries

The results presented here are based on the data taken during the energy scans in 1990 and 1991 with centre-of-mass energies, $\sqrt{s}$, in a range $|\sqrt{s} - m_{\mathrm{Z}}| < 3$ GeV, the high statistics data collected at the Z peak in 1992 and a preliminary analysis of the high precision scan in 1993. During this scan more than 18 pb^{-1} were recorded by each experiment at two centre-of-mass energy points roughly 1.8 GeV above and below the Z mass while about 15 pb^{-1} was within 200 MeV of m_{Z}. We also add several preliminary results based on data of the 1994 running period in which the LEP machine delivered approximately 65 pb^{-1} to each of the four LEP experiments at the Z peak.

The total statistics and the systematic errors of the individual LEP collaborations are given in Tables 1 and 2. Details of the individual analyses can be found in References 24–27. An important aspect of the lineshape analysis is a precise knowledge of the LEP centre-of-mass energies. The treatment of the LEP centre-of-mass energies by the four LEP experiments is based on [2]. For the

1994 data a preliminary LEP energy calibration is available [28]. In order to determine the Z mass, $m_{\rm Z}$, and the total Z width, $\Gamma_{\rm Z}$, all of the recorded data are combined, taking the energy uncertainty from the 1993 data to be uncorrelated with the energy uncertainty coming from previous years, resulting in an overall LEP energy error on $m_{\rm Z}$ of $\approx$1.5 MeV and on $\Gamma_{\rm Z}$ of $\approx$1.7 MeV.

For the averaging of results the LEP experiments provide a standard set of 9 parameters describing the information contained in hadronic and leptonic cross sections and leptonic forward-backward asymmetries [1,29]. These parameters are convenient for fitting and averaging since they have minimal correlations amongst themselves. They are:

- The mass of the Z, $m_{\rm Z}$, and the total width, $\Gamma_{\rm Z}$, where the definition is based on the Breit Wigner denominator $(s - m_{\rm Z}^2 + is\Gamma_{\rm Z}/m_{\rm Z})$ [30].
- The hadronic pole cross section:
$$\sigma_{\rm h}^0 \equiv \frac{12\pi}{m_{\rm Z}^2}\frac{\Gamma_{\rm ee}\Gamma_{\rm had}}{\Gamma_{\rm Z}^2}.$$
Here $\Gamma_{\rm ee}$ and $\Gamma_{\rm had}$ are the partial widths of the Z for decays into electrons and hadrons.
- The ratios:
$$R_{\rm e} \equiv \Gamma_{\rm had}/\Gamma_{\rm ee} \qquad R_\mu \equiv \Gamma_{\rm had}/\Gamma_{\mu\mu} \qquad R_\tau \equiv \Gamma_{\rm had}/\Gamma_{\tau\tau}. \tag{1}$$
Here $\Gamma_{\mu\mu}$ and $\Gamma_{\tau\tau}$ are the partial widths of the Z for the decays $\rm Z \to \mu^+\mu^-$ and $\rm Z \to \tau^+\tau^-$. Even under the assumption of lepton universality a small (0.2%) difference between the values for $R_{\rm e}$ and R_μ, and the value for R_τ due to mass corrections to $\Gamma_{\tau\tau}$ is expected.
- The pole asymmetries, $A_{\rm FB}^{0,\rm e}$, $A_{\rm FB}^{0,\mu}$ and $A_{\rm FB}^{0,\tau}$ for the processes $\rm e^+e^- \to e^+e^-$, $\rm e^+e^- \to \mu^+\mu^-$ and $\rm e^+e^- \to \tau^+\tau^-$. In terms of the effective vector and axial-vector neutral current couplings of fermions, g_{Vf} and g_{Af}, the pole asymmetries are expressed as:[1]
$$A_{\rm FB}^{0,\rm f} \equiv \frac{3}{4}\mathcal{A}_{\rm e}\mathcal{A}_{\rm f} \tag{2}$$
with:
$$\mathcal{A}_{\rm f} \equiv \frac{2g_{Vf}g_{Af}}{g_{Vf}^2 + g_{Af}^2}. \tag{3}$$

Note, that these parameters do not describe the Z production and decay completely, because they do not include the interference of the Z exchange with the photon exchange. This contribution is investigated in a separate note [31]. For the results presented in this Section, the γZ interference terms are fixed to their Standard Model values.

The four sets of 9 parameters provided by the LEP experiments are presented in Table 3. The covariance matrix of these parameters is as described in our previous paper [29]. It is constructed from the covariance matrices of the individual LEP experiments and common systematic errors. These common errors arise from the theoretical uncertainty in the luminosity normalization affecting the hadronic pole cross section, $\Delta\sigma_{\rm h}^0/\sigma_{\rm h}^0 = 0.16\%$, from the uncertainty of the LEP centre-of-mass energy spread of 5 MeV, resulting in $\Delta\Gamma_{\rm Z} \approx 1.0$ MeV, and from the uncertainty in the LEP energy calibration, giving $\Delta m_{\rm Z} \approx 1.5$ MeV, $\Delta\Gamma_{\rm Z} \approx 1.7$ MeV, and $\Delta A_{\rm FB}^{0,\ell} \approx 0.0005$ for each lepton species ($\ell = \rm e, \mu, \tau$). Full correlation between $A_{\rm FB}^{0,\mu}$ and $A_{\rm FB}^{0,\tau}$ and full anti-correlation between $A_{\rm FB}^{0,\rm e}$ and $A_{\rm FB}^{0,\mu}$ or $A_{\rm FB}^{0,\tau}$ is used. This change of sign of the energy effect for $A_{\rm FB}^{0,\rm e}$ is an approximation of the effect of the t-channel interference

[1] Effects coming from photon exchange, as well as real and imaginary parts of the photon vacuum polarization are not included in the definition of $A_{\rm FB}^{0,\rm f}$, but are accounted for explicitly in the fitting formulae used by the experiments.

for a typical LEP experimental acceptance for the e^+e^- final state. The combined parameter set and its correlation matrix are given in Tables 4 and 5.

If lepton universality is assumed, the set of 9 parameters given above is reduced to a set of 5 parameters. R_ℓ is defined as $R_\ell \equiv \Gamma_{\rm had}/\Gamma_{\ell\ell}$, where $\Gamma_{\ell\ell}$ refers to the partial Z width for the decay into a pair of massless charged leptons.

The data of each of the four LEP experiments are consistent with lepton universality (the χ^2/d.o.f. are $6/4, 4/4, 4/4$ and $5/4$ for ALEPH, DELPHI, L3 and OPAL, respectively). Based on this assumption Table 6 provides the five parameters $m_{\rm Z}$, $\Gamma_{\rm Z}$, $\sigma^0_{\rm h}$, R_ℓ and $A^{0,\ell}_{\rm FB}$ for the individual LEP experiments. The four experiments all use the above definition of $\Gamma_{\ell\ell}$. Tables 7 and 8 provide the five parameters $m_{\rm Z}$, $\Gamma_{\rm Z}$, $\sigma^0_{\rm h}$, R_ℓ and $A^{0,\ell}_{\rm FB}$ and the corresponding correlation matrix for the combined result of the 4 LEP experiments. Figure 1 shows, for each lepton species and for the combination assuming lepton universality, the resulting 68% probability contours in the R_ℓ-$A^{0,\ell}_{\rm FB}$ plane.

For completeness, in Table 9 the partial decay widths of the Z boson are listed. Note, that the substantial improvement of $\Gamma_{\ell\ell}$ as compared to [1] is essentially due to a decrease of systematic errors on both, the LEP energy calibration and the theoretical calculation of the small angle Bhabha cross section.

		ALEPH	DELPHI	L3	OPAL	LEP
$q\bar{q}$	'90-'91	451	356	416	454	1677
	'92	680	697	678	733	2788
	'93 prel.	640	677	654	646	2617
	'94 prel.	1281	[b]1144	1362	1524	5311
	total	3052	2874	3110	3357	12393
$\ell^+\ell^-$	'90-'91	55	37	40	58	190
	'92	82	69	58	88	297
	'93 prel.	78	71	61	82	292
	'94 prel.	[a]155	[b]54	123	184	516
	total	370	231	282	412	1295

Table 1: The LEP statistics in units of 10^3 events used for the analysis of the Z line shape and lepton forward-backward asymmetries.
[a]Statistics used in the measurement of the lepton cross section. The statistics used in the lepton forward-backward asymmetries is about 27% higher.
[b]Only part of the 1994 data set is included here. The results for leptons are for the $\mu^+\mu^-$ channel only.

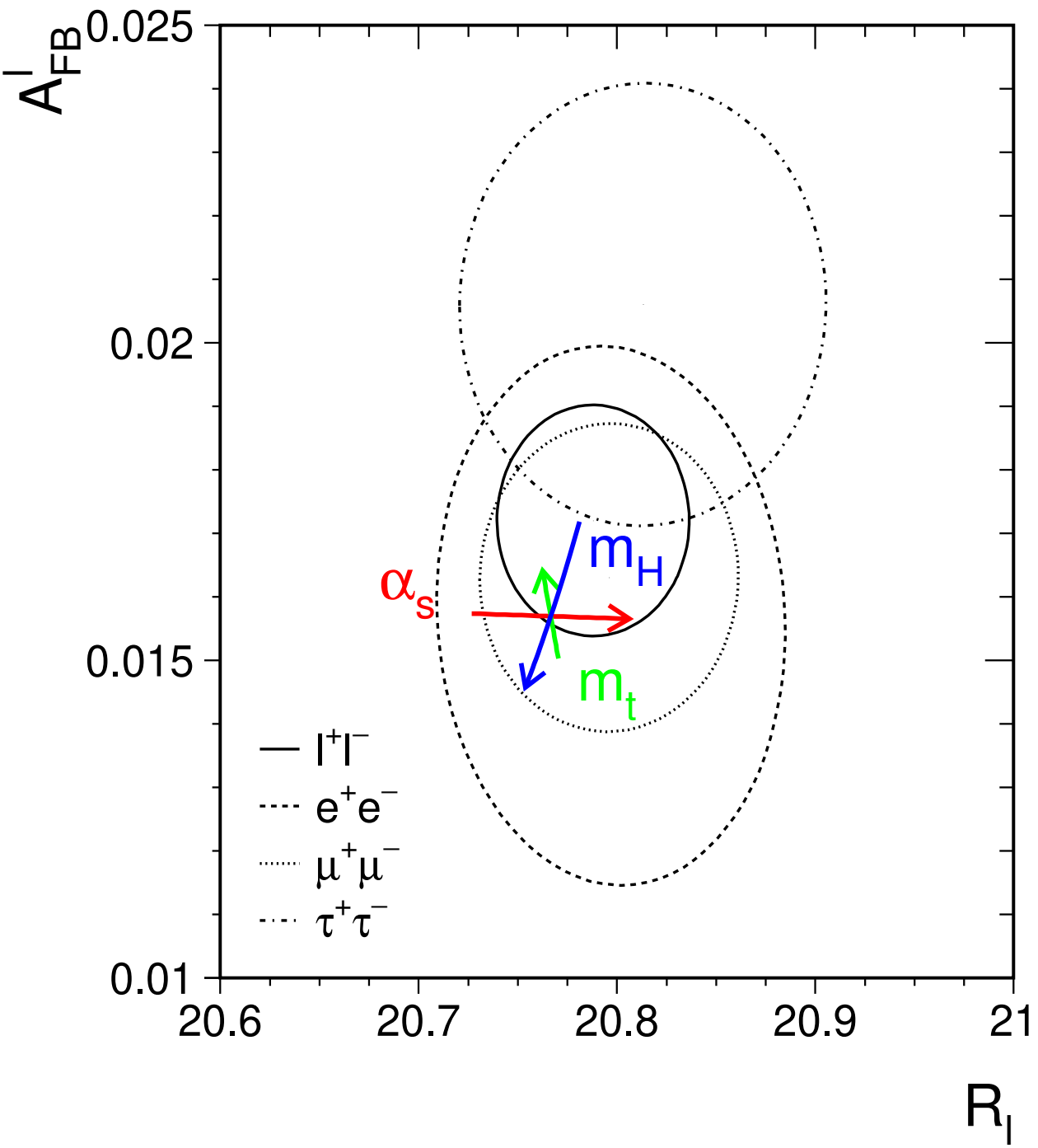

Figure 1: 68% probability contours in the R_ℓ-$A_{\rm FB}^{0,\ell}$ plane. Also shown is the Standard Model prediction for $m_{\rm Z} = 91.1884$ GeV, $m_{\rm t} = 180$ GeV, $m_{\rm H} = 300$ GeV, and $\alpha_s = 0.123$. The lines with arrows correspond to the variation of the Standard Model prediction when $m_{\rm t}$, $m_{\rm H}$ or $\alpha_s(m_{\rm Z}^2)$ are varied in the intervals $m_{\rm t} = 180 \pm 12$ GeV, $60 < m_{\rm H}({\rm GeV}) < 1000$ and $\alpha_s(m_{\rm Z}^2) = 0.123 \pm 0.006$, respectively. The arrows point in the direction of increasing values for $m_{\rm t}$, $m_{\rm H}$ and α_s.

	ALEPH		DELPHI		L3		OPAL	
	'93 prel.	'94 prel.	'93 prel.	'94 prel.	'93 prel.	'94 prel.	'93 prel.	'94 prel.
$\mathcal{L}^{\text{exp.}}$ [b]	0.087%	0.116%	0.21%	0.09%	0.12%	0.15%	0.076%	0.079%
σ_{had}	0.073%	0.073%	0.13%	0.15%	0.08%	0.2%	0.15%	0.16%
σ_{e}	0.50 %	0.48%	0.44%	[a]	0.3%	0.4%	0.23%	0.24%
σ_{μ}	0.25 %	0.26%	0.28%	0.40%	0.3%	0.6%	0.16%	0.15%
σ_{τ}	0.34 %	0.32%	0.8%	[a]	0.8%	1.5%	0.43%	0.46%
$A_{\text{FB e}}$	0.003	0.003	0.0026	[a]	0.004	0.004	0.0016	0.0016
$A_{\text{FB }\mu}$	0.001	0.001	0.0009	0.0015	0.001	0.002	0.001	0.001
$A_{\text{FB }\tau}$	0.004	0.004	0.0023	[a]	0.004	0.006	0.002	0.002

Table 2: The experimental systematic errors for the analysis of the Z line shape and lepton forward-backward asymmetries at the Z peak. The errors quoted do not include the common uncertainty due to the LEP energy calibration. The treatment of correlations between the errors for different years is described in References 24–27.
[a] No preliminary result quoted yet.
[b] In addition, there is a theoretical error for the calculation of the small angle Bhabha cross section of 0.16%, which has been treated as common to all experiments. The DELPHI theoretical error for 1993 is 0.17%.

	ALEPH	DELPHI	L3	OPAL
m_{Z}(GeV)	91.1924±0.0037	91.1849±0.0034	91.1936±0.0036	91.1852±0.0036
Γ_{Z}(GeV)	2.4954±0.0056[a]	2.4913±0.0053[a]	2.5022±0.0053[a]	2.4960±0.0052[a]
σ^0_{h}(nb)	41.56±0.09	41.39±0.10	41.48±0.11	41.47±0.10
R_e	20.54±0.11	20.88±0.16	20.89±0.12	20.90±0.10
R_μ	20.88±0.09	20.70±0.09	20.80±0.11	20.796±0.073
R_τ	20.77±0.10	20.61±0.16	20.73±0.17	21.00±0.11
$A^{0,\text{e}}_{\text{FB}}$	0.0196±0.0044	0.0233±0.0070	0.0125±0.0070	0.0081±0.0051
$A^{0,\mu}_{\text{FB}}$	0.0189±0.0029	0.0166±0.0030	0.0168±0.0038	0.0137±0.0027
$A^{0,\tau}_{\text{FB}}$	0.0206±0.0039	0.0210±0.0057	0.0287±0.0064	0.0183±0.0035
χ^2/d.o.f.	181/185	151/135	118/138	10/6[b]

Table 3: Line shape and asymmetry parameters from 9-parameter fits to the data of the four LEP experiments.
[a] Γ_{Z} has an additional error of 0.0010 GeV due to an uncertainty of 5 MeV in the LEP centre-of-mass energy spread which is common to all experiments.
[b] This parameter set has been obtained from a parameter transformation applied to the 15 parameters of the OPAL fit [27], which treats the γZ interference terms for leptons as additional free parameters. The extra parameters for the γZ interference terms have been fixed to their Standard Model values in the transformation. The χ^2/d.o.f. for the 15 parameter fit to the data is 87/132.

Parameter	Average Value
$m_{\rm Z}$(GeV)	91.1885±0.0022
$\Gamma_{\rm Z}$(GeV)	2.4963±0.0030 ± 0.0010
$\sigma^0_{\rm h}$(nb)	41.488±0.078
$R_{\rm e}$	20.797±0.058
R_μ	20.796±0.043
R_τ	20.813±0.061
$A^{0,\,{\rm e}}_{\rm FB}$	0.0157±0.0028
$A^{0,\,\mu}_{\rm FB}$	0.0163±0.0016
$A^{0,\,\tau}_{\rm FB}$	0.0206±0.0023

Table 4: Average line shape and asymmetry parameters from the data of the four LEP experiments given in Table 3, without the assumption of lepton universality. The χ^2/d.o.f. of the average is 36.1/27.

	$m_{\rm Z}$	$\Gamma_{\rm Z}$	$\sigma^0_{\rm h}$	$R_{\rm e}$	R_μ	R_τ	$A^{0,\,{\rm e}}_{\rm FB}$	$A^{0,\,\mu}_{\rm FB}$	$A^{0,\,\tau}_{\rm FB}$
$m_{\rm Z}$	1.00	−0.08	0.02	0.03	−0.02	−0.01	0.02	0.07	0.04
$\Gamma_{\rm Z}$	−0.08	1.00	−0.12	−0.01	0.00	0.00	0.00	0.00	0.00
$\sigma^0_{\rm h}$	0.02	−0.12	1.00	0.08	0.12	0.08	0.01	0.00	0.00
$R_{\rm e}$	0.03	−0.01	0.08	1.00	0.08	0.03	−0.06	0.01	0.01
R_μ	−0.02	0.00	0.12	0.08	1.00	0.06	0.00	0.01	0.00
R_τ	−0.01	0.00	0.08	0.03	0.06	1.00	0.00	0.00	0.01
$A^{0,\,{\rm e}}_{\rm FB}$	0.02	0.00	0.01	−0.06	0.00	0.00	1.00	−0.04	−0.02
$A^{0,\,\mu}_{\rm FB}$	0.07	0.00	0.00	0.01	0.01	0.00	−0.04	1.00	0.07
$A^{0,\,\tau}_{\rm FB}$	0.04	0.00	0.00	0.01	0.00	0.01	−0.02	0.07	1.00

Table 5: The correlation matrix for the set of parameters given in Table 4.

	ALEPH	DELPHI	L3	OPAL
$m_{\rm Z}$(GeV)	91.1924±0.0037	91.1849±0.0034	91.1938±0.0036	91.1846±0.0035
$\Gamma_{\rm Z}$(GeV)	2.4951±0.0055$^{(a)}$	2.4913±0.0053$^{(a)}$	2.5022±0.0053$^{(a)}$	2.4959±0.0052$^{(a)}$
$\sigma^0_{\rm h}$(nb)	41.56±0.09	41.40±0.10	41.48±0.11	41.47±0.10
R_ℓ	20.739±0.060	20.708±0.073	20.811±0.076	20.851±0.059
$A^{0,\,\ell}_{\rm FB}$	0.0195±0.0021	0.0182±0.0025	0.0186±0.0030	0.0142±0.0020
χ^2/d.o.f.	187/189	155/139	122/142	15/10$^{(b)}$

Table 6: Line shape and asymmetry parameters from 5-parameter fits to the data of the four LEP experiments, assuming lepton universality.
$^{(a)}\Gamma_{\rm Z}$ has an additional error of 0.0010 GeV due to an uncertainty of 5 MeV in the LEP centre-of-mass energy spread which is common to all experiments.
$^{(b)}$This parameter set has been obtained from a parameter transformation to the 15 parameters of the OPAL fit, which treats the γZ interference terms for leptons as additional free parameters.

Parameter	Average Value
$m_{\rm Z}$(GeV)	91.1884±0.0022
$\Gamma_{\rm Z}$(GeV)	2.4963±0.0030 ± 0.0010
$\sigma^0_{\rm h}$(nb)	41.488±0.078
R_ℓ	20.788±0.032
$A^{0,\ell}_{\rm FB}$	0.0172±0.0012

Table 7: Average line shape and asymmetry parameters from the results of the four LEP experiments given in Table 6, assuming lepton universality. The χ^2/d.o.f. of the average is 39.3/31.

	$m_{\rm Z}$	$\Gamma_{\rm Z}$	$\sigma^0_{\rm h}$	R_ℓ	$A^{0,\ell}_{\rm FB}$
$m_{\rm Z}$	1.00	−0.08	0.02	0.00	0.08
$\Gamma_{\rm Z}$	−0.08	1.00	−0.12	−0.01	0.00
$\sigma^0_{\rm h}$	0.02	−0.12	1.00	0.15	0.01
R_ℓ	0.00	−0.01	0.15	1.00	0.00
$A^{0,\ell}_{\rm FB}$	0.08	0.00	0.01	0.00	1.00

Table 8: The correlation matrix for the set of parameters given in Table 7.

Without Lepton Universality:	
$\Gamma_{\rm ee}$(MeV)	83.92±0.17
$\Gamma_{\mu\mu}$(MeV)	83.92±0.23
$\Gamma_{\tau\tau}$(MeV)	83.85±0.29

With Lepton Universality:	
$\Gamma_{\ell\ell}$(MeV)	83.93±0.14
$\Gamma_{\rm had}$(MeV)	1744.8±3.0
$\Gamma_{\rm inv}$(MeV)	499.9±2.5

Table 9: Partial decay widths of the Z boson, derived from the results of the 9-parameter (Tables 4 and 5) and the 5-parameter fit (Tables 7 and 8).

3 The τ Polarization

3.1 Introduction

The τ polarization $\mathcal{P}_\tau$ is determined by an indirect measurement of the longitudinal polarization of τ pairs produced in Z decays. It is defined as:

$$\mathcal{P}_\tau \equiv \frac{\sigma_R - \sigma_L}{\sigma_R + \sigma_L}\,, \tag{4}$$

where σ_R and σ_L are the τ-pair cross sections for the production of a right-handed and left-handed τ^-, respectively.

Neglecting small corrections for the effects of photon exchange and the γZ interference and electromagnetic radiative corrections for initial and final state radiation, all of which are taken into account in the analyses, the angular distribution of $\mathcal{P}_\tau$ as a function of the angle θ between the e^- and the τ^-, for $\sqrt{s} = m_{\rm Z}$ is given by:

$$\mathcal{P}_\tau(\cos\theta) = -\frac{\mathcal{A}_\tau + \mathcal{A}_{\rm e}\frac{2\cos\theta}{1+\cos^2\theta}}{1 + \mathcal{A}_\tau\mathcal{A}_{\rm e}\frac{2\cos\theta}{1+\cos^2\theta}}\,, \tag{5}$$

with $\mathcal{A}_{\rm e}$ and $\mathcal{A}_\tau$ defined in equation (3). When averaged over all production angles $\mathcal{P}_\tau$ is a measurement of $\mathcal{A}_\tau$, while as a function of $\cos\theta$, $\mathcal{P}_\tau(\cos\theta)$ provides nearly independent determinations of both $\mathcal{A}_\tau$ and $\mathcal{A}_{\rm e}$, allowing thus a test of the universality of the couplings of the Z to e and τ.

Each experiment makes separate $\mathcal{P}_\tau$ measurements using the five τ decay modes $e\nu\overline{\nu}$, $\mu\nu\overline{\nu}$, $\pi\nu$, $\rho\nu$ and $a_1\nu$ [32–35]. The $\rho\nu$ and $\pi\nu$ are the most sensitive channels, contributing weights of about 40% each in the average. In addition, DELPHI have used an inclusive hadronic analysis. The combination is made on the results from each experiment already averaged over the τ decay modes measured by the experiment.

A discussion of the effects of possible common systematic errors between the experiments can be found in [1].

3.2 Results

Tables 10 and 11 show the most recent results for $\mathcal{A}_\tau$ and $\mathcal{A}_{\rm e}$ obtained by the four experiments [32–35] and their combination. No common systematics are included in these averages. For further discussion see [1]. The statistical correlation between the extracted values of $\mathcal{A}_\tau$ and $\mathcal{A}_{\rm e}$ is small ($\leq 4\%$).

The average values for $\mathcal{A}_\tau$ and $\mathcal{A}_{\rm e}$:

$$\mathcal{A}_\tau = 0.1418 \pm 0.0075\,, \tag{6}$$

$$\mathcal{A}_{\rm e} = 0.1390 \pm 0.0089\,, \tag{7}$$

are compatible, as is expected from lepton universality. Assuming lepton universality, the values for $\mathcal{A}_\tau$ and $\mathcal{A}_{\rm e}$ can be combined. This combination is performed neglecting any possible common systematic error between $\mathcal{A}_\tau$ and $\mathcal{A}_{\rm e}$ within a given experiment. Such errors are estimated to be small, but warrant further study. The combined result of $\mathcal{A}_\tau$ and $\mathcal{A}_{\rm e}$ gives:

$$\mathcal{A}_\ell = 0.1406 \pm 0.0057\,. \tag{8}$$

For the future, further study of the uncertainties from the effects of radiative corrections for the ρ decay-mode of the τ is desirable.

ALEPH	('90 - '92), final	$0.136 \pm 0.012 \pm 0.009$
DELPHI	('90 - '92), final	$0.148 \pm 0.017 \pm 0.014$
L3	('90 - '94), prel.	$0.152 \pm 0.010 \pm 0.009$
OPAL	('90 - '94), prel.	$0.134 \pm 0.010 \pm 0.009$
LEP Average		0.1418 ± 0.0075

Table 10: LEP results for $\mathcal{A}_\tau$. The χ^2/d.o.f. for the average is 1.1/3

ALEPH	('90 - '92), final	$0.129 \pm 0.016 \pm 0.005$
DELPHI	('90 - '92), final	$0.136 \pm 0.027 \pm 0.003$
L3	('90 - '94), prel.	$0.156 \pm 0.016 \pm 0.005$
OPAL	('90 - '94), prel.	$0.134 \pm 0.015 \pm 0.004$
LEP Average		0.1390 ± 0.0089

Table 11: LEP results for $\mathcal{A}_e$. The χ^2/d.o.f. for the average is 1.5/3

4 Electroweak Results with b and c Quarks

4.1 Introduction

The relevant quantities measured at LEP in the heavy quark sector are:

- The ratios of the b and c quark partial widths to the total hadronic partial width: $R_{\mathrm{b}} \equiv \Gamma_{\mathrm{b\bar{b}}}/\Gamma_{\mathrm{had}}$ and $R_{\mathrm{c}} \equiv \Gamma_{\mathrm{c\bar{c}}}/\Gamma_{\mathrm{had}}$.
- The forward-backward asymmetries, $A_{\mathrm{FB}}^{\mathrm{b\bar{b}}}$ and $A_{\mathrm{FB}}^{\mathrm{c\bar{c}}}$.
- The semileptonic branching ratios, BR(b $\rightarrow \ell$) and BR(b $\rightarrow$ c $\rightarrow \ell^+$), and the average $\mathrm{B^0\overline{B^0}}$ mixing parameter, $\overline{\chi}$. These are often determined at the same time as the widths or asymmetries in multiparameter fits to lepton tag samples. They are included in the combination procedure to take into account their significant correlations with the other parameters.

The asymmetries vary rapidly with centre-of-mass energy [36]. In a first fit the asymmetry measurements on-peak, above peak and below peak have therefore been combined separately. The results of this fit are given in [36]. The centre-of-mass energy dependence of the measured asymmetries agrees with the one predicted by the Standard Model. To derive the coupling parameters and the electroweak mixing angle ($\sin^2\theta_{\mathrm{eff}}^{\mathrm{lept}}$) from the quark asymmetries, in a second fit all off-peak asymmetries have been transported to the peak energy before the fit. In this note only results from this last fit are quoted. There are therefore a total of 7 parameters to be determined in the combination procedure: the two partial widths, two asymmetries, two semileptonic branching ratios and the average mixing parameter.

Recently the SLD collaboration has presented precise measurements on R_{b} and on the left-right forward-backward asymmetry for b and c quarks. Since the precision and the dominant sources of systematic uncertainty are similar at LEP and SLC it is useful to produce combined LEP+SLD average. The left-right forward-backward asymmetries are, contrary to the unpolarized asymmetries, only sensitive to the final state couplings ($\mathcal{A}_{\mathrm{b}}$ and $\mathcal{A}_{\mathrm{c}}$) and will be considered as physically independent quantities. However the methods to measure the polarized and unpolarized asymmetries are very similar and thus the systematic uncertainties are potentially correlated. In order to obtain the exact correlation between the SLD and the LEP asymmetries $\mathcal{A}_{\mathrm{b}}$and $\mathcal{A}_{\mathrm{c}}$have been added as additional free parameters and measurements to the averaging procedure.

4.2 Summary of measurements and averaging procedure

Since the Summer of 1994, several preliminary analyses have now been published, and some new preliminary results including more data have become available. More details of the methods are given in the notes [1, 36–39]. For the combined fit of LEP+SLD measurements, last results from SLD have been taken into account. The measurements currently included in the combination are [36]:

- Lepton fits from all four LEP experiments [40–44].
- Event shape tag for R_{b} from ALEPH and L3 [45, 46].
- Lifetime (and lepton) double tag measurements for R_{b} from ALEPH, DELPHI, OPAL and SLD [12, 47–49].

- Measurements of $A_{FB}^{b\bar{b}}$ based on lifetime tagged events with a hemisphere charge measurement from ALEPH , DELPHI and OPAL where the the mean b-hemisphere charge is derived from the charge distributions themselves [42, 50, 51].

- Analyses with $D/D^{*\pm}$ mesons to measure R_c from DELPHI and OPAL [52,53], including for the first time double tag techniques.

- Analyses with a $D^{*\pm}$ meson to measure $A_{FB}^{c\bar{c}}$ and $A_{FB}^{b\bar{b}}$ from ALEPH, DELPHI and OPAL [42, 54, 55].

- Measurements of $\mathcal{A}_b$and $\mathcal{A}_c$from SLD [13–16]

These measurements are provided in the form of standard tables [36–39, 56] by the LEP and SLD collaborations. These tables include a detailed breakdown of the systematic error of each measurement and its dependence on other electroweak parameters. Where necessary, the experiments apply small corrections to their results in order to use agreed values and ranges for the input parameters used to calculate systematic errors. The measurements, corrected where necessary, are summarized in the Appendix in Tables 21-30, where the statistical and systematic errors are quoted separately. The correlated systematic entries are from sources shared with one or more other results in the table and are derived from the full breakdown of common systematic uncertainties. The uncorrelated systematic entries are from the remaining sources.

The χ^2 minimization procedure used to derive the values of all the parameters listed in Section 4.1 was unchanged [1, 36, 39, 56]. The explicit dependences of each measurement on the other parameters was taken into account, for example the dependence of the value of R_b on the assumed value of R_c as described below. The full statistical and systematic covariance matrix for all the measurements was calculated. The correlation matrices relating several measurements made in the same analyses were used, in particular for the multiparameter lepton fits. Additional correlations arising from common sources of systematic uncertainty were estimated from a detailed breakdown of systematic errors [36]. This breakdown for the double-tag measurements of R_b, plus the L3 event shape analysis which also measures this single parameter, is given for illustration in Table 12.

Since c-quark events form the main background in the R_b analyses, the value of R_b depends on the value of R_c. If R_b and R_c are measured in the same analysis, this is reflected in the correlation matrix for the results. Otherwise, this dependence may be written as:

$$R_b = R_b^{meas} + a(R_c)\frac{(R_c - R_c^{used})}{R_c}. \tag{9}$$

In this expression, R_b^{meas} is the result of the analysis which assumed a value of $R_c = R_c^{used}$. The values of R_c^{used} and the coefficients $a(x)$ are given in Table 21 where appropriate. The dependences of all other measurements on other electroweak parameters are treated in the same way.

The results for $BR(b \to \ell)$ and $BR(b \to c \to \ell^+)$ are now considered to be much more reliable than for summer 94 for the following reasons:

- A sign error in the quoted semileptonic decay model uncertainty has been corrected [43].

- The complete dependences of all the measurements on $\overline{\chi}$, $BR(b \to \ell)$ and $BR(b \to c \to \ell^+)$ are now taken into account in the same way as their dependence on the other electroweak parameters.

	ALEPH shape [45]	ALEPH lifetime [47]	DELPHI multiple [48]	L3 shape [46]	OPAL multiple [49]	SLD lifetime [12]
Charm production	0.0	−0.85	−1.0	0.0	−0.94	−1.25
D^0 lifetime	0.0	−0.28	−0.2	0.0	−0.23	−0.24
D^+ lifetime	0.0	−0.36	−0.2	0.0	−0.29	−0.15
D_s lifetime	0.0	−0.22	−0.2	0.0	−0.17	−0.17
D decay multip.	0.0	−0.57	−0.4	0.0	−0.76	−1.80
BR(D→K^0)	0.0	0.0	+0.6	0.0	+0.59	0.0
$g \to b\bar{b}, c\bar{c}$	0.0	−0.33	−0.2	0.0	−0.46	−0.40
Long-lived light hadrons	0.0	−0.24	−0.4	0.0	−0.33	−0.09
BR($c \to \ell$)	+0.6	0.0	−0.2	0.0	−0.28	0.0
Semilept.mod. $c \to \ell$	−2.1	0.0	−0.2	0.0	−0.25	0.0
$\langle x_E(c) \rangle$	+0.8	−0.12	−0.4	+1.8	−0.75	−1.22
Semilept model $b \to \ell$	−1.3	0.0	+0.2	0.0	0.0	0.0
$\langle x_E(b) \rangle$	0.0	0.0	0.0	−3.1	0.0	0.0
Total corr. error	2.7	1.2	1.5	3.6	1.7	2.6

Table 12: Example of breakdown of the correlated systematic error for R_b from lifetime, multiple and shape double-tag measurements (in units of 10^{-3}). The sign is the sign of the correlation among the experiments.

4.3 Treatment of the LEP Asymmetry Measurements

A 7 parameter fit was made, in which the peak and off-peak asymmetries were corrected to $\sqrt{s}$ = 91.26 GeV, using the predicted dependence from ZFITTER [57].

After calculating the overall averages, the corrections described below were made to the combined on-peak asymmetries to derive the pole asymmetries. The input measured asymmetries are all corrected to full acceptance and use the thrust axis as an estimate of the quark direction before gluon radiation. To relate $\sin^2\theta_{\rm eff}$ to these numbers a few corrections that are summarized in Table 13 have to be applied:

- Energy shift to $\sqrt{s} = M_Z$ and QED corrections: The slope of the asymmetry around M_Z depends only on the axial coupling and the charge of the initial and final state fermions and is thus independent of the pole asymmetry itself. The corrections due to the energy shift and initial state radiation have been calculated using ZFITTER [57].

- QCD corrections: The QCD corrections using the thrust axis have been calculated recently by Djouadi, Lampe and Zerwas [58] in first order QCD including mass corrections. They have been found to be $A_{FB}^{QCD} = A_{FB}^{noQCD}(1 + c\frac{\alpha_s}{\pi})$ with $c = -0.87$ for charm and $c = -0.79$ for bottom quarks.
  Assuming $\alpha_s(m_Z^2) = 0.12$ and a scale of $\mu^2 = (m_Z/2)^2$ the correction factor is $1 - 0.034 \pm 0.004$ ($1 - 0.037 \pm 0.004$) for b (c) quarks where the error is deduced from a variation of the renormalization scale between $(m_Z/4)^2$ and m_Z^2.
  This result is valid under the assumption of a full acceptance. However it has not yet been studied carefully how far events with very hard gluon radiation contribute in the same way to the asymmetry measurement as two jet events. For that reason another 25% error is assigned to the size of the QCD correction.

- γ exchange, γZ interference: These very small corrections have again been calculated using ZFITTER.

The lifetime/jet-charge measurements of asymmetries take into account QCD effects as an inherent part of the analysis, but the measured asymmetries for the analyses using a lepton or $D^\star$ tag need to be corrected for the effects of QCD on the event thrust axis direction. So that the averages could be made at the same level, the jet-charge measurements were adjusted by hand so as to be consistent with the other asymmetry measurements (i.e. 0.0033 was subtracted from each of the three $A_{\rm FB}^{\rm b\bar{b}}(\rm pk)$ jet-charge measurements before averaging).

source	δA^b_{FB}	δA^c_{FB}
$\sqrt{s} = M_z$	–0.0013	–0.0034
QED corrections	+0.0041	+0.0104
QCD corrections	$+0.0033 \pm 0.0010$	$+0.0023 \pm 0.0007$
γ, γZ	–0.0003	–0.0008
total	$+0.0058 \pm 0.0010$	$+0.0085 \pm 0.0007$

Table 13: Corrections to be applied to the quark asymmetries. The corrections are to be understood as $A^0_{FB} = A^{meas}_{FB} + \sum_i (\delta A_{FB})_i$

4.4 Results

4.4.1 Results of the 7 parameter fit to LEP data

Using the full averaging procedure gives the following combined results for the electroweak parameters:

$$\begin{aligned} R_{\rm b} &= 0.2216 \pm 0.0017 \\ R_{\rm c} &= 0.1546 \pm 0.0074 \\ {\rm BR(b} \to \ell) &= (11.10 \pm 0.23)\% \\ {\rm BR(b} \to {\rm c} \to \ell^+) &= (7.78 \pm 0.37)\% \\ \overline{\chi} &= 0.1147 \pm 0.0062 \\ A_{\rm FB}^{\rm b\bar{b}}({\rm pk}) &= (9.41 \pm 0.30)\% \\ A_{\rm FB}^{\rm c\bar{c}}({\rm pk}) &= (6.40 \pm 0.58)\% \end{aligned}$$

With the χ^2/dof of $54.1/(68-7)$, and a correlation matrix:

	$R_{\rm b}$	$R_{\rm c}$	$Br(1)$	$Br(2)$	$\overline{\chi}$	$A_{\rm FB}^{\rm b\bar{b}}(\rm pk)$	$A_{\rm FB}^{\rm c\bar{c}}(\rm pk)$
$R_{\rm b}$	1.000	–.341	–.114	–.046	.015	.001	.061
$R_{\rm c}$	–.341	1.000	.020	.157	–.015	.085	–.066
$Br(1)$	–.114	.020	1.000	–.255	.185	–.023	.075
$Br(2)$	–.046	.157	–.255	1.000	–.309	–.068	–.174
$\overline{\chi}$	.015	–.015	.185	–.309	1.000	.327	–.004
$A_{\rm FB}^{\rm b\bar{b}}(\rm pk)$	.001	.085	–.023	–.068	.327	1.000	.101
$A_{\rm FB}^{\rm c\bar{c}}(\rm pk)$	.061	–.066	.075	–.174	–.004	.101	1.000

There is a correlation of –0.34 between $R_{\rm b}$ and $R_{\rm c}$. The total corrections for the on-peak asymmetries to give the pole asymmetries are $+0.0058 \pm 0.0010$ and $+0.0085 \pm 0.0007$ for b and c respectively. In

addition there is a correction of +0.0003 (–0.0003) to R_b (R_c) due to photon exchange. The main results to be used in electroweak fits are then:

$$\begin{aligned} R_b &= 0.2219 \pm 0.0017 \\ R_c &= 0.1543 \pm 0.0074 \\ A_{FB}^{0,b} &= 0.0999 \pm 0.0031 \\ A_{FB}^{0,c} &= 0.0725 \pm 0.0058 \end{aligned} \tag{10}$$

with their correlation matrix given in Table 14:

	R_b	R_c	$A_{FB}^{0,b}$	$A_{FB}^{0,c}$
R_b	1.000	–.341	.001	.061
R_c	–.341	1.000	.085	–.066
$A_{FB}^{0,b}$	.001	.085	1.000	.101
$A_{FB}^{0,c}$	.061	–.066	.101	1.000

Table 14:

If R_c is fixed to 0.172, then the value of R_b is: $R_b = 0.2205 \pm 0.0016$ ($R_c = 0.172$).

The pole forward-backward asymmetries are related to $\mathcal{A}_c$ and $\mathcal{A}_b$ by equation (2). Assuming lepton universality, the value of $\mathcal{A}_e = \mathcal{A}_\ell$ can be derived from the measured lepton forward-backward asymmetry:

$$A_{FB}^{0,\ell} = 0.0172 \pm 0.0012 \equiv \frac{3}{4}\mathcal{A}_\ell{}^2,$$

which gives:

$$\mathcal{A}_\ell = 0.1514 \pm 0.0053,$$

and from the tau polarization measurements, again assuming lepton universality:

$$\mathcal{A}_\ell = 0.1406 \pm 0.0057.$$

The average value of $\mathcal{A}_\ell$ is then:

$$\mathcal{A}_\ell = 0.1464 \pm 0.0039.$$

From the measured values of $A_{FB}^{0,b}$ and $A_{FB}^{0,c}$ this gives:

$$\begin{aligned} \mathcal{A}_b &= 0.910 \pm 0.037 \\ \mathcal{A}_c &= 0.660 \pm 0.056\,, \end{aligned}$$

in good agreement with the Standard Model prediction $\mathcal{A}_b = 0.935$ and $\mathcal{A}_c = 0.667$ ($m_Z = 91.1884$ GeV, $m_t = 180$ GeV, $m_H = 300$ GeV).

4.4.2 Results of the 9 parameter fit to LEP and SLD data

Including the SLD results on R_b , $\mathcal{A}_b$ and $\mathcal{A}_c$ into the fit the following results are obtained:

$$\begin{aligned} R_b &= 0.2216 \pm 0.0017 \\ R_c &= 0.1543 \pm 0.0074 \\ \mathrm{BR}(b \to \ell) &= (11.12 \pm 0.23)\% \end{aligned}$$

$$
\begin{aligned}
\mathrm{BR}(\mathrm{b} \to \mathrm{c} \to \ell^+) &= (7.76 \pm 0.36)\% \\
\overline{\chi} &= 0.1145 \pm 0.0061 \\
A_{\mathrm{FB}}^{\mathrm{b\bar{b}}}(\mathrm{pk}) &= (9.39 \pm 0.30)\% \\
A_{\mathrm{FB}}^{\mathrm{c\bar{c}}}(\mathrm{pk}) &= (6.44 \pm 0.58)\% \\
\mathcal{A}_{\mathrm{b}} &= 0.841 \pm 0.053 \\
\mathcal{A}_{\mathrm{c}} &= 0.606 \pm 0.090
\end{aligned}
$$

With the χ^2/dof of $55.1/(74-9)$, and a correlation matrix:

	R_{b}	R_{c}	$Br(1)$	$Br(2)$	$\overline{\chi}$	$A_{\mathrm{FB}}^{\mathrm{b\bar{b}}}(\mathrm{pk})$	$A_{\mathrm{FB}}^{\mathrm{c\bar{c}}}(\mathrm{pk})$	$\mathcal{A}_{\mathrm{b}}$	$\mathcal{A}_{\mathrm{c}}$
R_{b}	1.000	–.345	–.120	–.046	.020	.005	.055	–.068	.046
R_{c}	–.345	1.000	.023	.150	–.009	.084	–.063	.074	–.061
$Br(1)$	–.120	.023	1.000	–.255	.191	–.017	.068	–.002	.060
$Br(2)$	–.046	.150	–.255	1.000	–.299	–.066	–.171	–.069	–.096
$\overline{\chi}$	.020	–.009	.191	–.299	1.000	.322	–.001	.115	.016
$A_{\mathrm{FB}}^{\mathrm{b\bar{b}}}(\mathrm{pk})$	.005	.084	–.017	–.066	.322	1.000	.109	.062	–.025
$A_{\mathrm{FB}}^{\mathrm{c\bar{c}}}(\mathrm{pk})$	.055	–.063	.068	–.171	–.001	.109	1.000	–.018	.073
$\mathcal{A}_{\mathrm{b}}$	–.068	.074	–.002	–.069	.115	.062	–.018	1.000	.074
$\mathcal{A}_{\mathrm{c}}$	.046	–.061	.060	–.096	.016	–.025	.073	.074	1.000

The $\mathcal{A}_{\mathrm{b}}$ and $\mathcal{A}_{\mathrm{c}}$ values are already corrected for all QED and QCD effects. Correcting the LEP measurements for photon exchange etc. yields:

$$
\begin{aligned}
R_{\mathrm{b}} &= 0.2219 \pm 0.0017 \\
R_{\mathrm{c}} &= 0.1540 \pm 0.0074 \\
A_{\mathrm{FB}}^{0,\,\mathrm{b}} &= 0.0997 \pm 0.0031 \\
A_{\mathrm{FB}}^{0,\,\mathrm{c}} &= 0.0729 \pm 0.0058 \\
\mathcal{A}_{\mathrm{b}} &= 0.841 \pm 0.053 \\
\mathcal{A}_{\mathrm{c}} &= 0.606 \pm 0.090
\end{aligned}
\tag{11}
$$

with their correlation matrix given in Table 15:

	R_{b}	R_{c}	$A_{\mathrm{FB}}^{0,\,\mathrm{b}}$	$A_{\mathrm{FB}}^{0,\,\mathrm{c}}$	$\mathcal{A}_{\mathrm{b}}$	$\mathcal{A}_{\mathrm{c}}$
R_{b}	1.000	–.345	.005	.055	–.068	.046
R_{c}	–.345	1.000	.084	–.063	.074	–.061
$A_{\mathrm{FB}}^{0,\,\mathrm{b}}$	.005	.084	1.000	.109	.062	–.025
$A_{\mathrm{FB}}^{0,\,\mathrm{c}}$	.055	–.063	.109	1.000	–.018	.073
$\mathcal{A}_{\mathrm{b}}$	–.068	.074	.062	–.018	1.000	.074
$\mathcal{A}_{\mathrm{c}}$	.046	–.061	–.025	.073	.074	1.000

Table 15:

If R_{c} is fixed to 0.172, then the value of R_{b} is: $R_{\mathrm{b}} = 0.2205 \pm 0.0016$ ($R_{\mathrm{c}} = 0.172$).

It is not yet clear how to correlate the uncertainty in the QCD correction between the LEP and SLD results. In the numbers presented above they have been assumed to be independent. If one assumes this error to be fully correlated the correlation between $A_{\mathrm{FB}}^{0,\,\mathrm{b}}$ and $\mathcal{A}_{\mathrm{b}}$ would increase by 0.04 and the one $A_{\mathrm{FB}}^{0,\,\mathrm{c}}$ and $\mathcal{A}_{\mathrm{c}}$ would increase by 0.008. All other elements of the correlation matrix remain unchanged.

Combining LEP and SLD results, following the same method as in Section 4.4.1 to extract $\mathcal{A}_b$ and $\mathcal{A}_c$ from $A_{FB}^{0,b}$ and $A_{FB}^{0,c}$, but now also using the SLD left-right asymmetry measurement, A_{LR} [10,11], to constrain $\mathcal{A}_\ell$ results in:

$$\begin{aligned} \mathcal{A}_b &= 0.871 \pm 0.027 \\ \mathcal{A}_c &= 0.635 \pm 0.046. \end{aligned}$$

The agreement for $\mathcal{A}_b$ and $\mathcal{A}_c$ with the Standard Model prediction $\mathcal{A}_b = 0.935$ and $\mathcal{A}_c = 0.667$ ($m_Z = 91.1884$ GeV, $m_t = 180$ GeV, $m_H = 300$ GeV) is at the two and one standard deviation level, respectively.

5 The Hadronic Charge Asymmetry $\langle Q_{FB} \rangle$

ALEPH [59–61], DELPHI [62], and OPAL [63, 64] have provided measurements of $\sin^2\theta^{lept}_{eff}$ based on the mean difference in jet charges measured in the forward and backward event hemispheres, $\langle Q_{FB} \rangle$. DELPHI have also provided a related measurement of the total charge asymmetry by making a charge assignment on an event by event basis and performing a likelihood fit. The experimental values quoted for the average forward-backward charge difference $\langle Q_{FB} \rangle$, cannot be directly compared as some of them include detector dependent effects, acceptances and detector efficiencies. We therefore use $\sin^2\theta^{lept}_{eff}$ as a means of combining the results summarized in Table 16.

Exp.		$\sin^2\theta^{lept}_{eff}$
ALEPH	90-93 prel.	$0.2323 \pm 0.0010 \pm 0.0010$
DELPHI	90-91	$0.2345 \pm 0.0030 \pm 0.0027$
OPAL	91-94 prel.	$0.2326 \pm 0.0012 \pm 0.0013$
Average		0.2325 ± 0.0013

Table 16: Summary of the determination of $\sin^2\theta^{lept}_{eff}$ from inclusive hadronic charge asymmetries at LEP. For each experiment, the first error is statistical, the second systematic, which is dominated by the fragmentation and decay modelling uncertainties.

The dominant systematic error remains the modelling of the charge flow in the fragmentation process for each flavour. Both ALEPH and OPAL measure the required charge properties for $Z \to b\bar{b}$ events from the data. ALEPH have also determined the charm charge properties from the data. The JETSET fragmentation is used by all experiments as reference, the HERWIG model is used for comparison. The JETSET parameters are varied to estimate the systematic errors. The understanding of the allowed ranges for the parameters is improving with time, and various constraints to measured data distributions are imposed. The central values chosen by the experiments for these parameters are, however, not the same. The degree of correlation between the fragmentation uncertainties for the different experiments requires further investigation. For the moment we treat them as fully correlated. The present average of $\sin^2\theta^{lept}_{eff}$ is not very sensitive to the treatment of common uncertainties.

The ambiguities due to QCD corrections may cause changes in the derived value of $\sin^2\theta^{lept}_{eff}$, which are however well below the fragmentation and experimental errors. The estimated systematic uncertainties from this source are considered fully correlated between experiments.

There is also some correlation between these results and those for $A^{b\bar{b}}_{FB}$ using jet charges. The dominant source of correlation is again through uncertainties in the fragmentation and decay models used. The typical correlation between the derived values of $\sin^2\theta^{lept}_{eff}$ between the $\langle Q_{FB} \rangle$ and the $A^{b\bar{b}}_{FB}$ jet charge measurement has been estimated to be between 20 and 25%. This leads to only a small change in the relative weights for the $A^{b\bar{b}}_{FB}$ and $\langle Q_{FB} \rangle$ results when averaging their $\sin^2\theta^{lept}_{eff}$ values. Further, the jet charge method contributes at most half of the weight of the $A^{b\bar{b}}_{FB}$ measurement. Thus, the correlation between $\langle Q_{FB} \rangle$ and $A^{b\bar{b}}_{FB}$ from jet charge will have little impact on the overall Standard Model fit, and is neglected at present.

6 Interpretation of Results

6.1 The Effective Z Couplings

The partial widths of the Z into leptons and the lepton forward-backward asymmetries (Section 2), the τ polarization and the τ polarization asymmetry (Section 3) can all be combined to determine the effective vector and axial vector couplings for e, μ and τ. The asymmetries (Equations 2 and 5) determine the ratio $g_{V\ell}/g_{A\ell}$ (Equation 3), while the sum of the squares of the couplings is derived from the leptonic partial widths:

$$\Gamma_{\ell\ell} = \frac{G_{\rm F} m_{\rm Z}^3}{6\pi\sqrt{2}}(g_{V\ell}^2 + g_{A\ell}^2)(1 + \delta_\ell^{QED}) \,, \tag{12}$$

where $\delta_\ell^{QED} = 3q_\ell^2\alpha(m_{\rm Z}^2)/(4\pi)$ accounts for final state photonic corrections.

The averaged results for the effective lepton couplings are given in Table 17. Figure 2 shows the 68% probability contours in the $g_{A\ell}$-$g_{V\ell}$ plane. The signs of $g_{A\ell}$ and $g_{V\ell}$ are based on the convention $g_{A\rm e} < 0$. With this convention the signs of the couplings of all charged leptons follow from LEP data alone. For comparison, the measurement of $A_{\rm LR}$ from SLD [10,11] is indicated as a band in the $g_{A\ell}$-$g_{V\ell}$-plane of Figure 2, which shows an acceptable overlap with the LEP data. The information on the leptonic couplings from LEP can therefore be combined with the $A_{\rm LR}$ measurement of SLD. The results for this combination are given in the right column of Table 17. The measured ratios of the e, μ and τ couplings provide a test of lepton universality and are also given in Table 17.

	Without Lepton Universality:	
	LEP	LEP+SLC
$g_{V\rm e}$	-0.0368 ± 0.0017	-0.03850 ± 0.00087
$g_{V\mu}$	-0.0370 ± 0.0041	-0.0354 ± 0.0036
$g_{V\tau}$	-0.0371 ± 0.0018	-0.0369 ± 0.0018
$g_{A\rm e}$	-0.50115 ± 0.00052	-0.50103 ± 0.00051
$g_{A\mu}$	-0.50113 ± 0.00076	-0.50124 ± 0.00075
$g_{A\tau}$	-0.50151 ± 0.00089	-0.50152 ± 0.00089
	Ratios of couplings:	
	LEP	LEP+SLC
$g_{V\mu}/g_{V\rm e}$	1.01 ± 0.14	0.92 ± 0.10
$g_{V\tau}/g_{V\rm e}$	1.008 ± 0.071	0.959 ± 0.052
$g_{A\mu}/g_{A\rm e}$	1.0000 ± 0.0018	1.0004 ± 0.0018
$g_{A\tau}/g_{A\rm e}$	1.0007 ± 0.0020	1.0010 ± 0.0020
	With Lepton Universality:	
	LEP	LEP+SLC
$g_{V\ell}$	-0.0369 ± 0.0010	-0.03797 ± 0.00071
$g_{A\ell}$	-0.50119 ± 0.00041	-0.50111 ± 0.00041
g_ν	$+0.5011 \pm 0.0013$	$+0.5011 \pm 0.0013$

Table 17: Results for the effective vector and axial vector couplings derived from the combined LEP data without and with the assumption of lepton universality. For the right column the SLD measurement of $A_{\rm LR}$ is also included.

The neutrino couplings to the Z can be derived from the measured value of the invisible width of the Z, $\Gamma_{\rm inv}$, attributing it exclusively to the decay into three identical neutrino generations ($\Gamma_{\rm inv} = 3\Gamma_{\nu\nu}$)

and assuming $g_{A\nu} = g_{V\nu} \equiv g_\nu$. The relative sign of g_ν is chosen to be in agreement with neutrino scattering data [65], resulting in

$$g_\nu = +0.5011 \pm 0.0013.$$

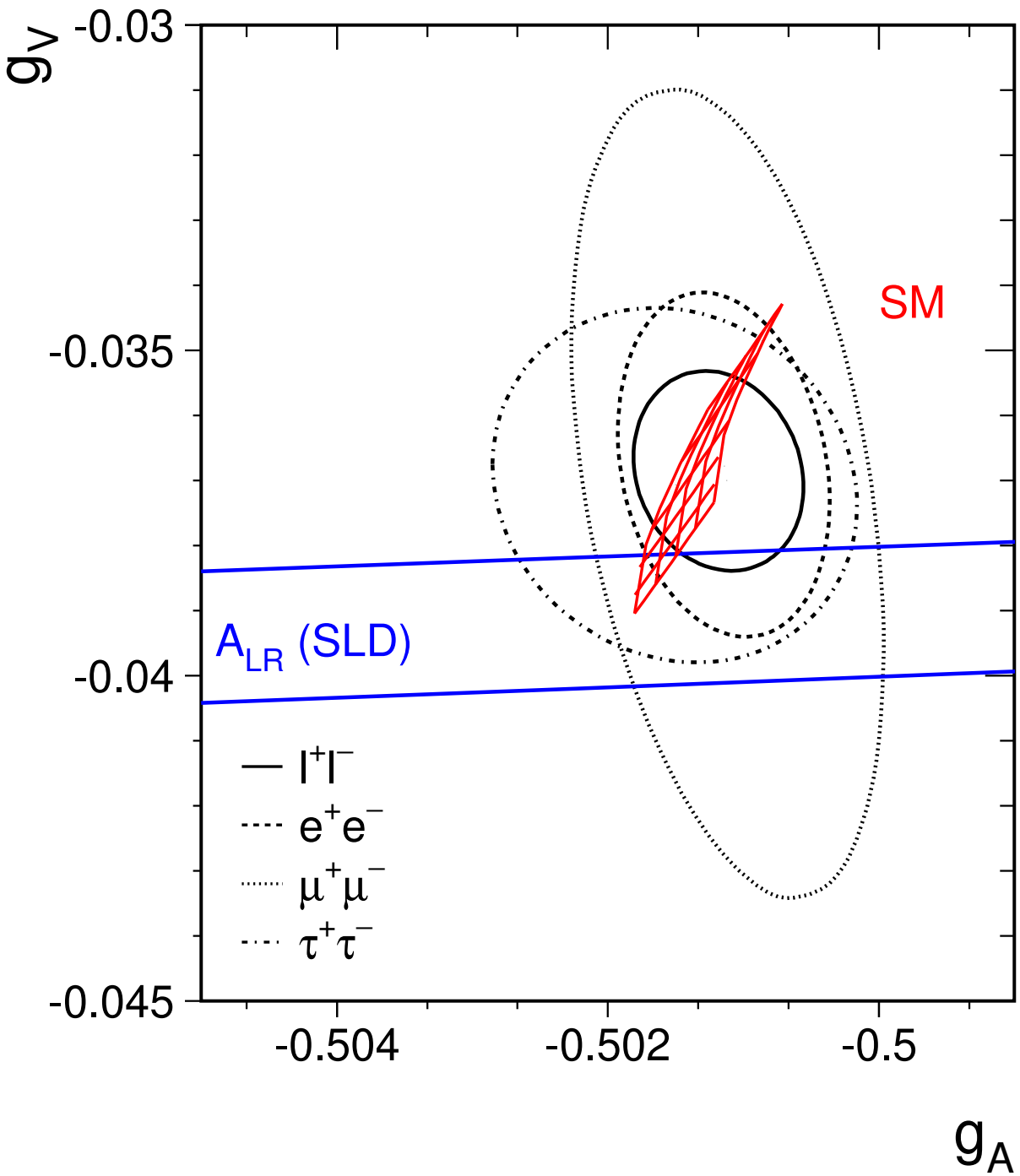

Figure 2: The 68% probability contours in the $g_{V\ell}$-$g_{A\ell}$ plane from LEP measurements. The solid contour results from a fit assuming lepton universality. Also shown is the one standard deviation band resulting from the $A_{\rm LR}$ measurement of SLD. The grid corresponds to the Standard Model prediction for $m_{\rm t} = 180 \pm 12$ GeV and $60 \leq m_{\rm H}$ [GeV] ≤ 1000.

6.2 The Effective Electroweak Mixing Angle $\sin^2\theta^{\rm lept}_{\rm eff}$

The asymmetry measurements from LEP can be combined into a single observable, the effective electroweak mixing angle, $\sin^2\theta^{\rm lept}_{\rm eff}$, defined as:

$$\sin^2\theta^{\rm lept}_{\rm eff} \equiv \frac{1}{4}(1 - g_{V\ell}/g_{A\ell})\,, \tag{13}$$

without making any strong model-specific assumptions.

For a combined average of $\sin^2\theta^{\rm lept}_{\rm eff}$ from $A^{0,\ell}_{\rm FB}$, $\mathcal{A}_\tau$ and $\mathcal{A}_{\rm e}$ only the assumption of lepton universality, already inherent in the definition of $\sin^2\theta^{\rm lept}_{\rm eff}$, is needed. In practice no further assumption is involved if the quark forward-backward asymmetries, $A^{\rm b\bar{b}}_{\rm FB}$ and $A^{\rm c\bar{c}}_{\rm FB}$, are included in this average, as these asymmetries have a reduced sensitivity to corrections particular to the hadronic vertex. The results of these determinations of $\sin^2\theta^{\rm lept}_{\rm eff}$ and their combination are shown in Table 18. Also the comparison with the measurement of the left-right asymmetry, $A_{\rm LR}$, at SLD [10, 11] is given. It should be noted that $A_{\rm LR}$ measures the same quantity as $\mathcal{A}_{\rm e}$ from τ polarization, with minimal model dependence. Both measurements have small systematic errors.

	$\sin^2\theta^{\rm lept}_{\rm eff}$	Average by Group of Observations	Cumulative Average	χ^2/d.o.f.
$A^{0,\ell}_{\rm FB}$	0.23096 ± 0.00068			
$\mathcal{A}_\tau$	0.23218 ± 0.00095			
$\mathcal{A}_{\rm e}$	0.2325 ± 0.0011	0.23160 ± 0.00049	0.23160 ± 0.00049	1.9/2
$A^{0,\rm b}_{\rm FB}$	0.23209 ± 0.00055			
$A^{0,\rm c}_{\rm FB}$	0.2318 ± 0.0013	0.23205 ± 0.00051	0.23182 ± 0.00035	2.4/4
$\langle Q_{\rm FB}\rangle$	0.2325 ± 0.0013	0.2325 ± 0.0013	0.23186 ± 0.00034	2.6/5
$A_{\rm LR}$ (SLD)	0.23049 ± 0.00050	0.23049 ± 0.00050	0.23143 ± 0.00028	7.8/6

Table 18: Comparison of several determinations of $\sin^2\theta^{\rm lept}_{\rm eff}$ from asymmetries. Averages are obtained as weighted averages assuming no correlations. The second column lists the $\sin^2\theta^{\rm lept}_{\rm eff}$ values derived from the quantities listed in the first column. The third column contains the averages of these numbers by groups of observations, where the groups are indicated by the horizontal lines. The last column shows the cumulative averages. The χ^2 per degree of freedom for the cumulative averages also is given.

6.3 Number of Neutrinos

An important aspect of our measurement concerns the information related to Z decays into invisible channels. Using the results of Tables 7 and 8 the ratio of the Z decay width into invisible particles and the leptonic decay width is determined:

$$\Gamma_{\rm inv}/\Gamma_{\ell\ell} \;=\; 5.956 \pm 0.031\,.$$

Dividing this by the Standard Model value for the ratio of the partial widths to neutrinos and charged leptons:

$$(\Gamma_{\nu\nu}/\Gamma_{\ell\ell})_{\rm SM} \;=\; 1.991 \pm 0.001\,,$$

where the central value is evaluated for $m_{\rm Z} = 91.1884$ GeV, $m_{\rm t} = 180$ GeV, $m_{\rm H} = 300$ GeV and the error quoted accounts for a variation of $m_{\rm t}$ in the range $m_{\rm t} = 180 \pm 12$ GeV and a variation of $m_{\rm H}$ in the range $60 < m_{\rm H}({\rm GeV}) < 1000$, the number of light neutrinos is found to be:

$$N_\nu \;\; = \;\; 2.991 \pm 0.016.$$

6.4 Standard Model Constraints

The precise electroweak measurements performed at LEP can be used to check the validity of the Standard Model and, within its framework, to infer valuable information about its basic parameters. Their accuracy makes them sensitive to the top quark mass, $m_{\rm t}$, and to the mass of the Higgs boson, $m_{\rm H}$, through the loop corrections. The leading top quark dependence is quadratic and allows a determination of $m_{\rm t}$. The main dependence on $m_{\rm H}$ is logarithmic and therefore, with the present data accuracy, the constraints on $m_{\rm H}$ are still weak.

The various LEP measurements are summarized in Table 19a and presented in Figure 3 and 4 together with their Standard Model prediction as a function of $m_{\rm t}$. The bands in the Standard Model predictions reflect the linear sum of the expected variations of each quantity due to a change of the strong coupling constant $\alpha_s(m_{\rm Z}^2) = 0.123 \pm 0.006$ [66] and $m_{\rm H}$ in the interval $60 \leq m_{\rm H}$ [GeV] ≤ 1000 for $m_{\rm Z} = 91.1884$ GeV.

Table 20 shows the constraints obtained on $m_{\rm t}$ and $\alpha_s(m_{\rm Z}^2)$ when fitting the measurements in Table 19 to up to date Standard Model calculations [68] as verified by the working group on 'Precision Calculations at LEP-I' [69]. The fits have been repeated for $m_{\rm H} = 60$, 300 and 1000 GeV and the difference in the fitted parameters is quoted as the second uncertainty. Shown in Table 20 are the results obtained using only LEP data (Table 19a), as well as those obtained by including preliminary results from the SLD collaboration (Table 19b) for the left-right asymmetry, $A_{\rm LR}$ [10,11], and electroweak measurements with heavy flavours ($R_{\rm b}$ [12], $\mathcal{A}_{\rm b}$ and $\mathcal{A}_{\rm c}$ [13–16]). Finally, the right-most column of Table 19 gives the Standard Model constraints obtained by including in addition the published measurements of $m_{\rm W}$ from UA2 [20], CDF [21,22] and a preliminary result for $m_{\rm W}$ from DØ [23][2], and the measurements of the neutrino neutral to charged current ratios from CDHS [17], CHARM [18] and CCFR [19] (Table 19c).

The χ^2/d.o.f. values for all these fits have probabilities ranging from 0.6% to 3.5%. The measurements of $R_{\rm b}$ and $R_{\rm c}$ cause a χ^2 contribution of approximately 15 for all the Standard Model fits in Table 20 (see also Table 19).

In the Standard Model both the measurement of $R_{\rm b}$ and $R_{\rm c}$ are not very sensitive to $m_{\rm t}$ and $\alpha_s(m_{\rm Z}^2)$ as compared to other input data of this analysis. If they are omitted from the fit the value of $m_{\rm t}$ increases by only 4 GeV, the value of $\alpha_s(m_{\rm Z}^2)$ stays approximately constant. The value of $\alpha_s(m_{\rm Z}^2)$ derived from an analysis of electroweak precision tests within the Standard Model framework depends essentially on R_ℓ, $\Gamma_{\rm Z}$ and $\sigma_{\rm h}^0$. The result is in very good agreement with that obtained from event shape measurements at LEP ($\alpha_s(m_{\rm Z}^2) = 0.123 \pm 0.006$ [66]) and of similar precision. The strong coupling constant can also be determined from the parameter R_ℓ alone. For $m_{\rm Z} = 91.1884$ GeV, and imposing $m_{\rm t} = 180 \pm 12$ GeV as constraint, $\alpha_s = 0.126 \pm 0.005 \pm 0.002$ is obtained, where the second error accounts for the variation of the result when varying $m_{\rm H}$ in $60 \leq m_{\rm H}$ [GeV] ≤ 1000.

There is a strong correlation (of -0.35) between the $R_{\rm b}$ and $R_{\rm c}$ measurements. If the value of $R_{\rm c}$ is fixed to the Standard Model value $R_{\rm c} = 0.172$, ignoring the pull of $R_{\rm c}$, the agreement between the

[2] See [67] for a combination of these $m_{\rm W}$ measurements.

	Measurement	Standard Model Fit	Pull
a) LEP			
line-shape and lepton asymmetries:			
m_Z [GeV]	91.1884 ± 0.0022	91.1882	0.1
Γ_Z [GeV]	2.4963 ± 0.0032	2.4973	−0.3
σ_h^0 [nb]	41.488 ± 0.078	41.450	0.5
R_ℓ	20.788 ± 0.032	20.773	0.5
$A_{FB}^{0,\ell}$	0.0172 ± 0.0012	0.0159	1.1
+ correlation matrix Table 8			
τ polarization:			
$\mathcal{A}_\tau$	0.1418 ± 0.0075	0.1455	−0.5
$\mathcal{A}_e$	0.1390 ± 0.0089	0.1455	−0.7
b and c quark results:			
R_b [a]	0.2219 ± 0.0017	0.2156	3.7
R_c [a]	0.1543 ± 0.0074	0.1724	−2.5
$A_{FB}^{0,b}$ [a]	0.0999 ± 0.0031	0.1020	−0.7
$A_{FB}^{0,c}$ [a]	0.0725 ± 0.0058	0.0728	0.0
+ correlation matrix Table 14			
$q\bar{q}$ charge asymmetry:			
$\sin^2\theta_{eff}^{lept}$ ($\langle Q_{FB} \rangle$)	0.2325 ± 0.0013	0.23172	0.6
b) SLC			
$\sin^2\theta_{eff}^{lept}$ (A_{LR} [10,11])	0.23049 ± 0.00050	0.23172	−2.5
R_b [12] [a]	0.2171 ± 0.0054	0.2156	0.3
$\mathcal{A}_b$ [13–16]	0.841 ± 0.053	0.935	−1.8
$\mathcal{A}_c$ [13–16]	0.606 ± 0.090	0.667	−0.7
c) $p\bar{p}$ and νN			
m_W [GeV] ($p\bar{p}$ [67])	80.26 ± 0.16	80.35	−0.5
$1 - m_W^2/m_Z^2$ (νN [17–19])	0.2257 ± 0.0047	0.2237	0.4

Table 19: Summary of measurements included in the combined analysis of Standard Model parameters. Section a) summarizes LEP averages, Section b) SLD results for $\sin^2\theta_{eff}^{lept}$ from the measurement of the left-right polarization asymmetry, for R_b and for $\mathcal{A}_b$ and $\mathcal{A}_c$ from polarized forward-backward asymmetries and Section c) electroweak precision tests from $p\bar{p}$ colliders and νN-scattering. The Standard Model fit results in column 3 and the pulls (difference between measurement and fit in units of the measurement error) in column 4 are derived from the fit including all data (Table 20, column 4) for a fixed value of $m_H = 300$ GeV.
[a] For fits which combine LEP and SLD heavy flavour measurements we use as input the heavy flavour results given in eqn. (11) and their correlation matrix in Table 15 in Section 4 of this note.

R_b measurement and the Standard Model fit result improves from 3.7 to 3.2 standard deviations. In this case one obtains $R_b = 0.2205 \pm 0.0016$.

	LEP	LEP + SLD	LEP + SLD + $p\overline{p}$ and νN data
m_t (GeV)	$170 \pm 10\ ^{+17}_{-19}$	$180\ ^{+8\ +17}_{-9\ -20}$	$178 \pm 8\ ^{+17}_{-20}$
$\alpha_s(m_Z^2)$	$0.125 \pm 0.004\ \pm 0.002$	$0.123 \pm 0.004\ \pm 0.002$	$0.123 \pm 0.004\ \pm 0.002$
χ^2/d.o.f.	18/9	28/12	28/14
$\sin^2\theta_{\rm eff}^{\rm lept}$	$0.23206 \pm 0.00028\ ^{+0.00008}_{-0.00017}$	$0.23166 \pm 0.00025\ ^{+0.00006}_{-0.00013}$	$0.23172 \pm 0.00024\ ^{+0.00007}_{-0.00014}$
$1 - m_W^2/m_Z^2$	$0.2247 \pm 0.0010\ ^{+0.0004}_{-0.0002}$	$0.2234 \pm 0.0009\ ^{+0.0005}_{-0.0002}$	$0.2237 \pm 0.0009\ ^{+0.0004}_{-0.0002}$
m_W (GeV)	$80.295 \pm 0.057\ ^{+0.011}_{-0.019}$	$80.359 \pm 0.051\ ^{+0.013}_{-0.024}$	$80.346 \pm 0.046\ ^{+0.012}_{-0.021}$

Table 20: Results of fits to LEP and other electroweak precision data for m_t and $\alpha_s(m_Z^2)$. No external constraint on $\alpha_s(m_Z^2)$ has been imposed. The second column presents the results obtained using LEP data only (Table 19a). The third column gives the result when the SLD measurements of the left-right asymmetry and electroweak heavy flavour results (Table 19b) are also added. In the fourth column also the combined data from the $p\overline{p}$ collider and νN experiments (Table 19c) are included. The central values and the first errors quoted refer to $m_H = 300$ GeV. The second errors correspond to the variation of the central value when varying m_H in the interval $60 \leq m_H\ [\mathrm{GeV}] \leq 1000$. The bottom part of the table lists derived results for $\sin^2\theta_{\rm eff}^{\rm lept}$, $1 - m_W^2/m_Z^2$ and m_W.

Attributing the deviation of R_b to new physics in the b partial width, R_ℓ should also be affected since $\Gamma_{b\bar{b}}$ is a component of the total hadronic width [70]. In Figure 5 the measured value of R_b is plotted versus $\sin^2\theta_{\rm eff}^{\rm lept}$. If one assumes the Standard Model dependence on $\sin^2\theta_{\rm eff}^{\rm lept}$ for the light quark widths and taking $\alpha_s(m_Z^2) = 0.123 \pm 0.006$, R_ℓ imposes a constraint on the two variables. The one-sigma R_ℓ band is centred on the Standard Model prediction while the R_b band is off-set. The overlap, however, depends on the value of $\alpha_s(m_Z^2)$.

Various fits are performed to combine the full set of data in Table 19 allowing extra contributions beyond the Standard Model predictions to $\Gamma_{b\bar{b}}$ and $\Gamma_{c\bar{c}}$. In a first example, the $b\overline{b}$ partial width is parametrized as $\Gamma_{b\bar{b}} = \Gamma_{b\bar{b}}(SM) + X_b$, where $\Gamma_{b\bar{b}}(SM)$ refers to the Standard Model value of $\Gamma_{b\bar{b}}$ and X_b represents a new extra contribution. The extra contribution X_b is also propagated to all observables which depend on the hadronic width. The results of this fit are $X_b = 11.7 \pm 3.8 \pm 1.4$ MeV, $\alpha_s(m_Z^2) = 0.102 \pm 0.008$, $m_t = 181 \pm 8^{+17}_{-19}$ GeV, with a χ^2/d.o.f. of 18/13. In a second example, $\Gamma_{c\bar{c}}$ is also parametrized as $\Gamma_{c\bar{c}} = \Gamma_{c\bar{c}}(SM) + X_c$, where the extra contributions X_b and X_c are treated simultaneously as free parameters. This fit has a χ^2/d.o.f. of 13/12 and the resulting value of $\alpha_s(m_Z^2)$ is $\alpha_s(m_Z^2) = 0.18 \pm 0.04$.

In any extension of the Standard Model where QCD corrections to quark partial widths are essentially universal[3], the values of R_b and R_c are also insensitive to $\alpha_s(m_Z^2)$. These additional measurements, however, probe our understanding of quark partial widths which is crucial for the determination of $\alpha_s(m_Z^2)$ from electroweak precision tests. The value of $\alpha_s(m_Z^2)$ determined from R_ℓ, Γ_Z and σ_h^0 depends on the clarification of the puzzle imposed by the additional measurements of R_b and R_c. The relative errors of $\Gamma_{c\bar{c}}$ and $\Gamma_{b\bar{b}}$ are still large as compared to that of Γ_{had}. It is therefore premature to draw a conclusion on the value of $\alpha_s(m_Z^2)$ in any extension of the Standard Model.

As shown above, the value of m_t resulting from the Standard Model fits is robust, whatever

[3] In the Standard Model small deviations from universality are due to the interplay of QCD, electroweak and mass corrections.

interpretation is given to the measurement of R_b and R_c. This is to be expected as the constraint on m_t comes mainly from the leptonic sector. For example, Figure 6 shows a comparison of the leptonic partial width from LEP, $\Gamma_{\ell\ell}$, and the the effective electroweak mixing angle from asymmetries measured at LEP and SLC, $\sin^2\theta^{lept}_{eff}$, with the Standard Model. Good agreement with the Standard Model prediction is observed. The star shows the prediction if among the electroweak radiative corrections only the photon vacuum polarization is included, showing evidence that LEP data are sensitive to genuinely electroweak corrections. The fitted value of m_t is in excellent agreement with the top mass values $m_t = 176 \pm 8$ (stat.) $\pm$ 10 (syst.) GeV and $m_t = 199^{+19}_{-21}$ (stat.) $\pm$ 22 (syst.) GeV reported from the observation of the top quark at the TEVATRON by the CDF [8] and the DØ collaborations [9], respectively. For the sake of comparison with electroweak precision data the weighted average of both measurements, $m_t = 180 \pm 12$ GeV, is used in this note.

Figure 7 shows the χ^2 value for the Standard Model fits discussed in Table 20 column 4, as a function of m_t for the three values of m_H (60, 300 and 1000 GeV) considered. It can be seen that the minima of these curves occur at different values of χ^2. This suggests the possibility of extracting constraints on the value of m_H.

The main m_H dependence of the Standard Model predictions for the measurements listed in Table 19 is given by corrections proportional to $\log(m_H)$. The effects of m_H and m_t, however, are correlated for most observables, which weakens the determination of m_H without a direct measurement of m_t. Figure 8 shows the observed value of $\Delta\chi^2 \equiv \chi^2 - \chi^2_{min}$ as a function of m_H, when the Tevatron value of m_t is used as an additional constraint in the fit. The observed $\Delta\chi^2$ curve exhibits a minimum for low values of m_H. The $\Delta\chi^2 = 2.7$ interval, approximately corresponding to a 95% confidence level upper limit, extends up to 500 GeV.

Detailed studies of the theoretical uncertainties in the Standard Model predictions due to missing higher order electroweak corrections and their interplay with QCD corrections are carried out in the working group on 'Precision calculations for the Z resonance' [69]. Theoretical uncertainties are evaluated there by comparing different but within our present knowledge equivalent treatments of aspects like resummation techniques, momentum transfer scales for vertex corrections and factorization schemes. The impact of these intrinsic theoretical uncertainties on m_t and $\alpha_s(m_Z^2)$ has been estimated as the maximal variation of the fitted parameters when the Standard Model fits in this Section to the input data in Table 19 are repeated using several combinations of options which were implemented in the electroweak libraries used [68] for the study performed in [69]. As a result the value of m_t for the Standard Model fits presented in this Section varies by $\Delta m_t \leq 2$ GeV and the value of $\alpha_s(m_Z^2)$ by $\Delta\alpha_s(m_Z^2) \leq 0.001$. The error of $\alpha_s(m_Z^2)$ covers missing higher order electroweak corrections and uncertainties in the interplay of electroweak and QCD corrections but not the effect of missing higher order QCD corrections. A complete discussion of theoretical uncertainties in the determination of α_s from R_ℓ can be found in [71].

At present the impact of theoretical uncertainties on the determination of m_t from precise electroweak measurements is small compared to the uncertainty in the value of $\alpha(m_Z^2)$ due to the contribution of light quarks to the photon vacuum-polarization. Recently there have been several reevaluations of $\alpha(m_Z^2)$ [4–7]. For the results presented in this Section, a value of $\alpha(m_Z^2) = 1/(128.896 \pm 0.090)$ [6] is used, where the error is propagated in the fits. This uncertainty causes an error of 0.00023 on the Standard Model prediction of $\sin^2\theta^{lept}_{eff}$ and an error of 4 GeV on m_t. The effect on the Standard Model prediction for $\Gamma_{\ell\ell}$ is negligible. The $\alpha_s(m_Z^2)$ values quoted in Table 20 are stable against a variation of $\alpha(m_Z^2)$ in the interval quoted.

Acknowledgements
We thank members of the CCFR, CDF, D0 and SLD Collaborations for making results available to us

in advance of the conferences and for useful discussions concerning their combination. In particular, we would like to thank Su Dong, J. Huber and B. Schumm from the SLD Collaboration for providing a break-down of the systematic uncertainties in their heavy flavour analyses in a form which allowed a consistent combination with the LEP results.

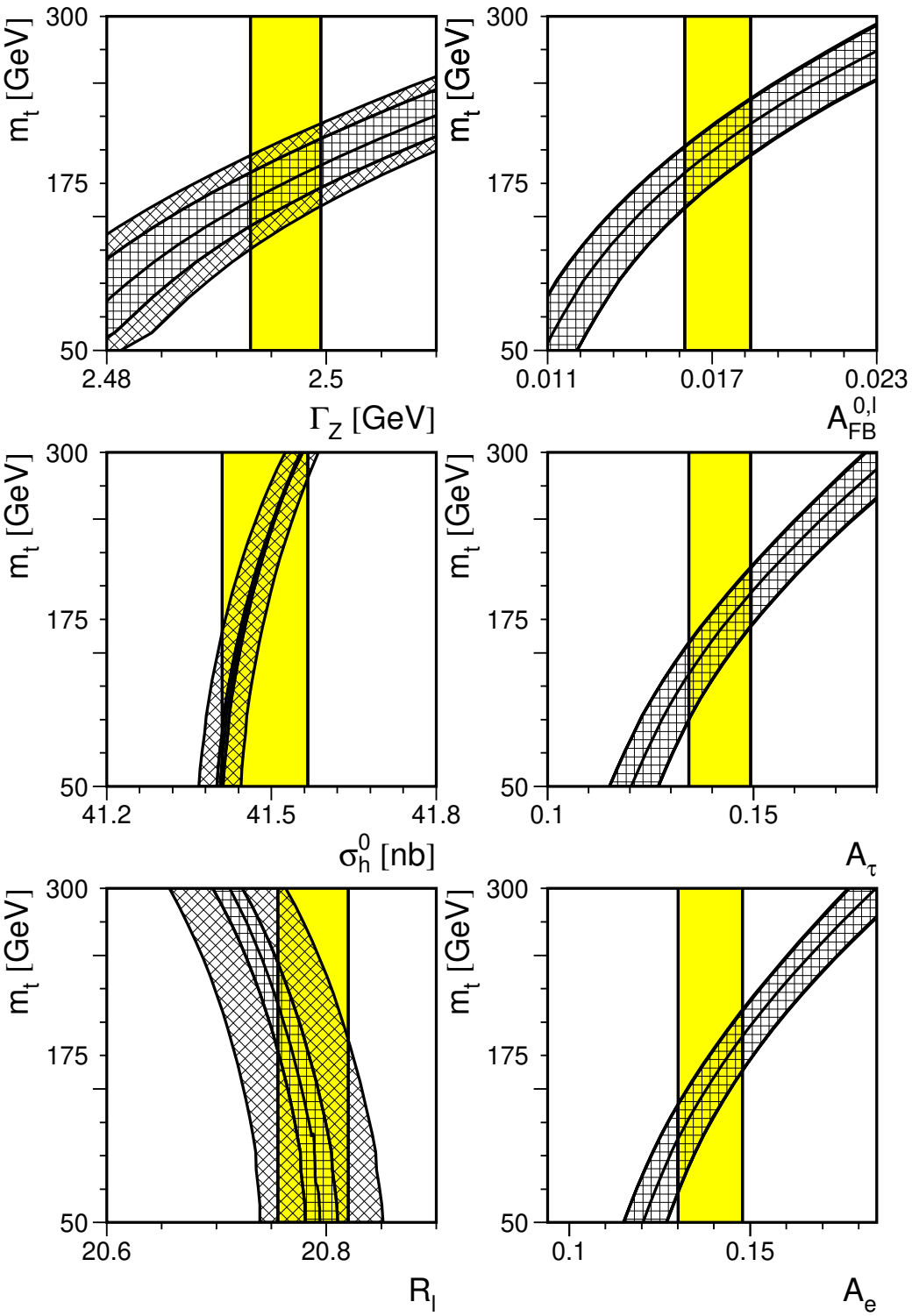

Figure 3: Comparison of LEP measurements with the Standard Model prediction as a function of m_t. The cross-hatch pattern parallel to the axes indicates the variation of the Standard Model prediction with m_H spanning the interval $60 < m_H\,(\mathrm{GeV}) < 1000$ and the slant cross-hatch pattern corresponds to a variation of $\alpha_s(m_Z^2)$ within the interval $\alpha_s(m_Z^2) = 0.123 \pm 0.006$. The total width of the band corresponds to the linear sum of both uncertainties. The experimental errors on the parameters are indicated as vertical bands.

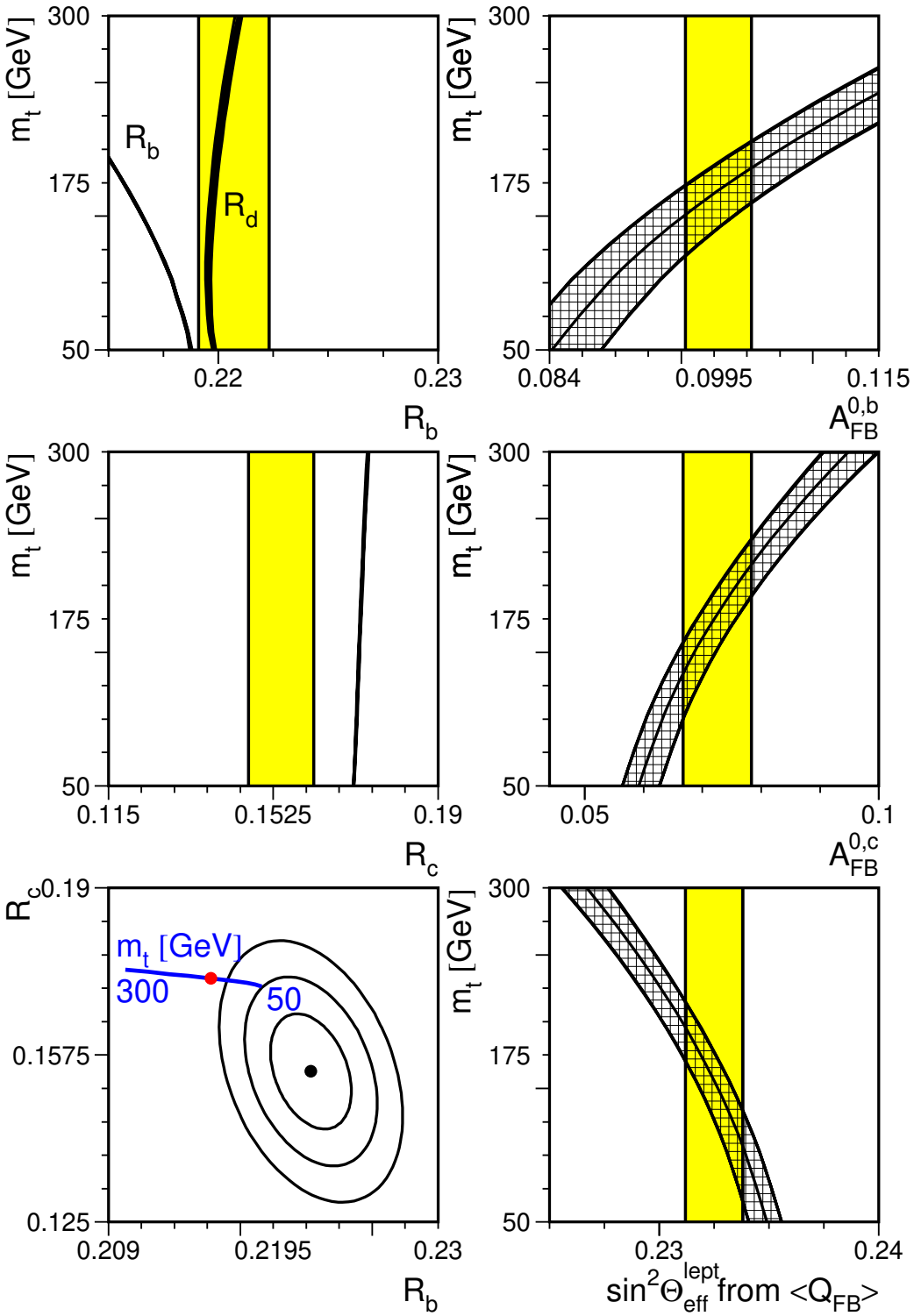

Figure 4: Comparison of LEP measurements with the Standard Model prediction as a function of m_t (*c.f.* Figure 3). For ratios of hadronic partial widths this variation with m_H and $\alpha_s(m_Z^2)$ nearly cancels. For the comparison of R_b with the Standard Model the value of R_c has been fixed to the Standard Model. Also shown are the 68%, 95% and 99.7% confidence level contours in the R_b-R_c plane together with the Standard Model prediction. To illustrate the impact of special vertex corrections to R_b the Standard Model prediction of R_d is also indicated.

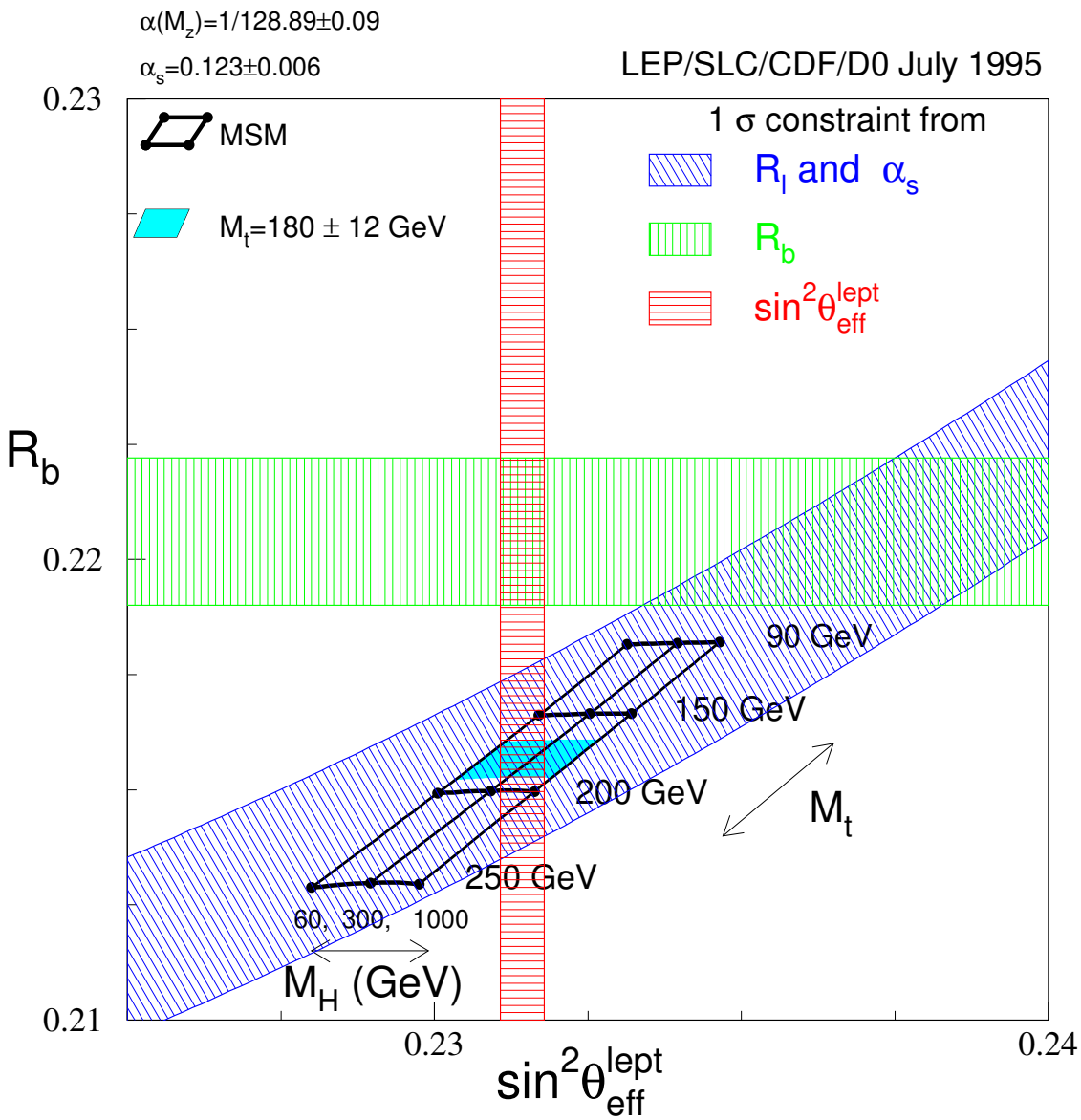

Figure 5: The LEP/SLD measurements of $\sin^2\theta^{\rm lept}_{\rm eff}$ and $R_{\rm b}$ and the Standard Model prediction. Also shown is the constraint resulting from the measurement of R_ℓ on these variables, assuming $\alpha_s(m_{\rm Z}^2) = 0.123 \pm 0.006$, as well as the Standard Model dependence of light quark partial widths on $\sin^2\theta^{\rm lept}_{\rm eff}$.

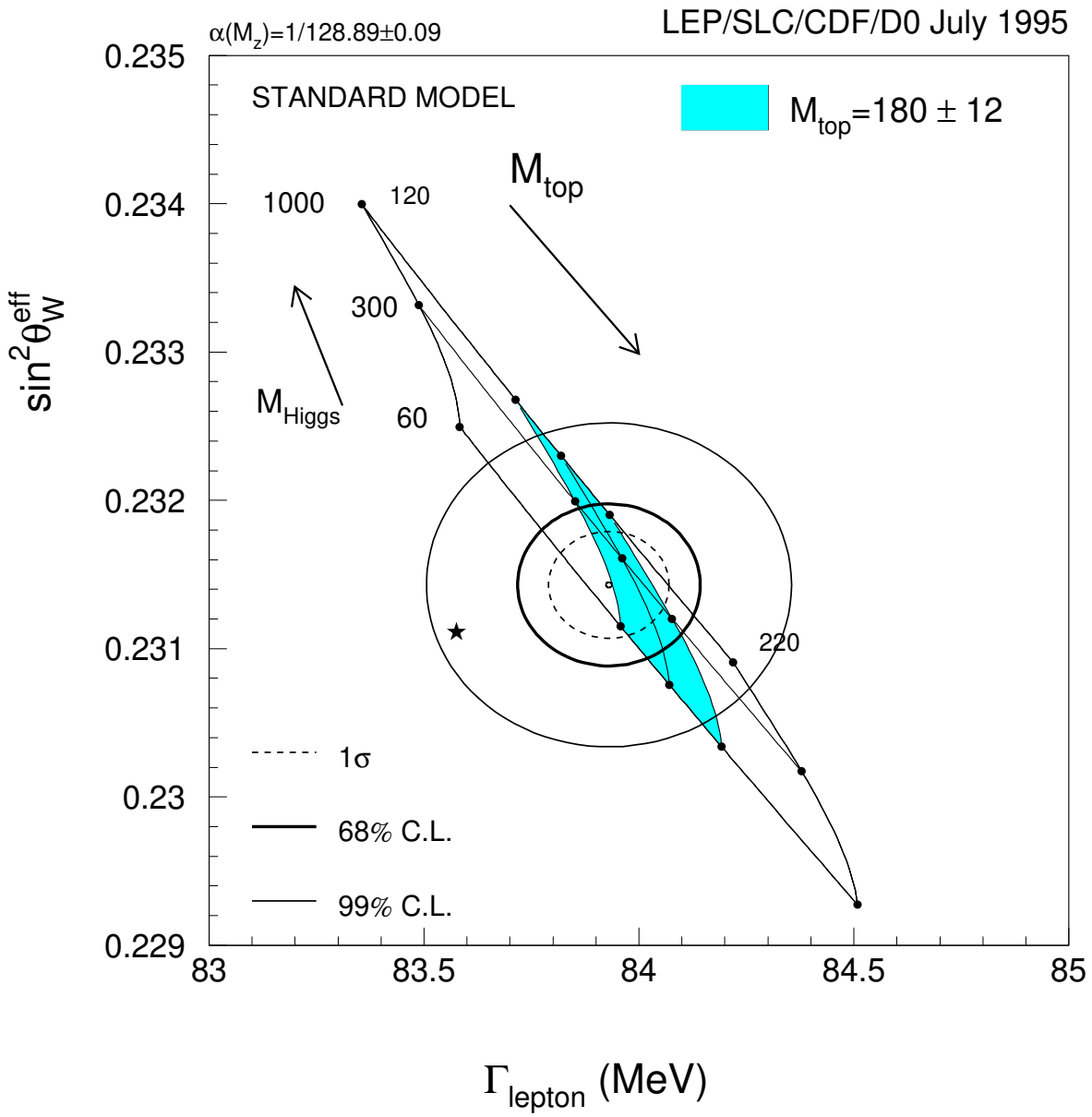

Figure 6: The LEP/SLD measurements of $\sin^2\theta^{\rm lept}_{\rm eff}$ and $\Gamma_{\ell\ell}$ and the Standard Model prediction. The star shows the predictions if among the electroweak radiative corrections only the photon vacuum polarization is included.

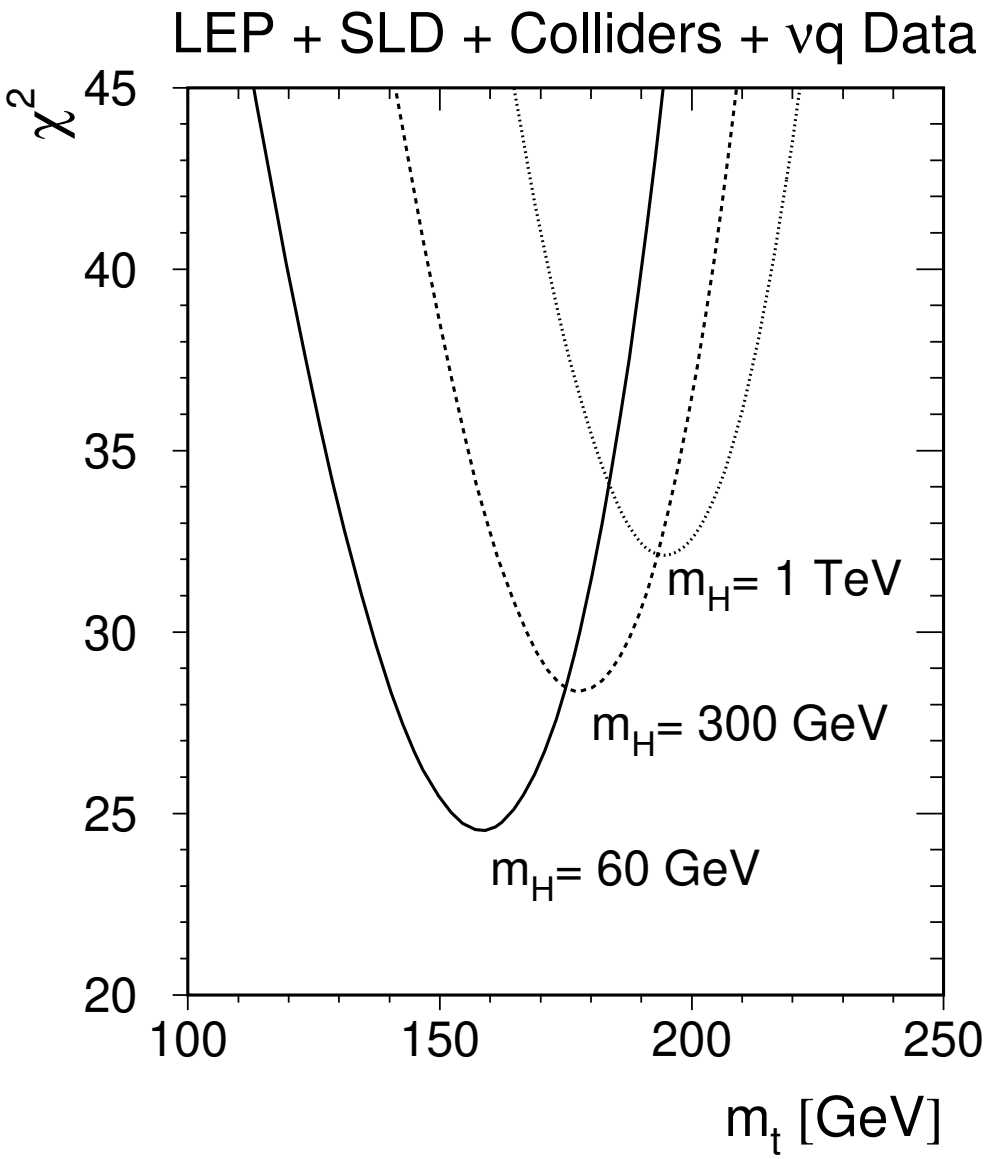

Figure 7: The χ^2 curves for the Standard Model fit in Table 20, column 4 to the electroweak precision measurements listed in Table 19 as a function of $m_{\rm t}$ for three different Higgs mass values spanning the interval $60 \leq m_{\rm H}\,[\mathrm{GeV}] \leq 1000$.

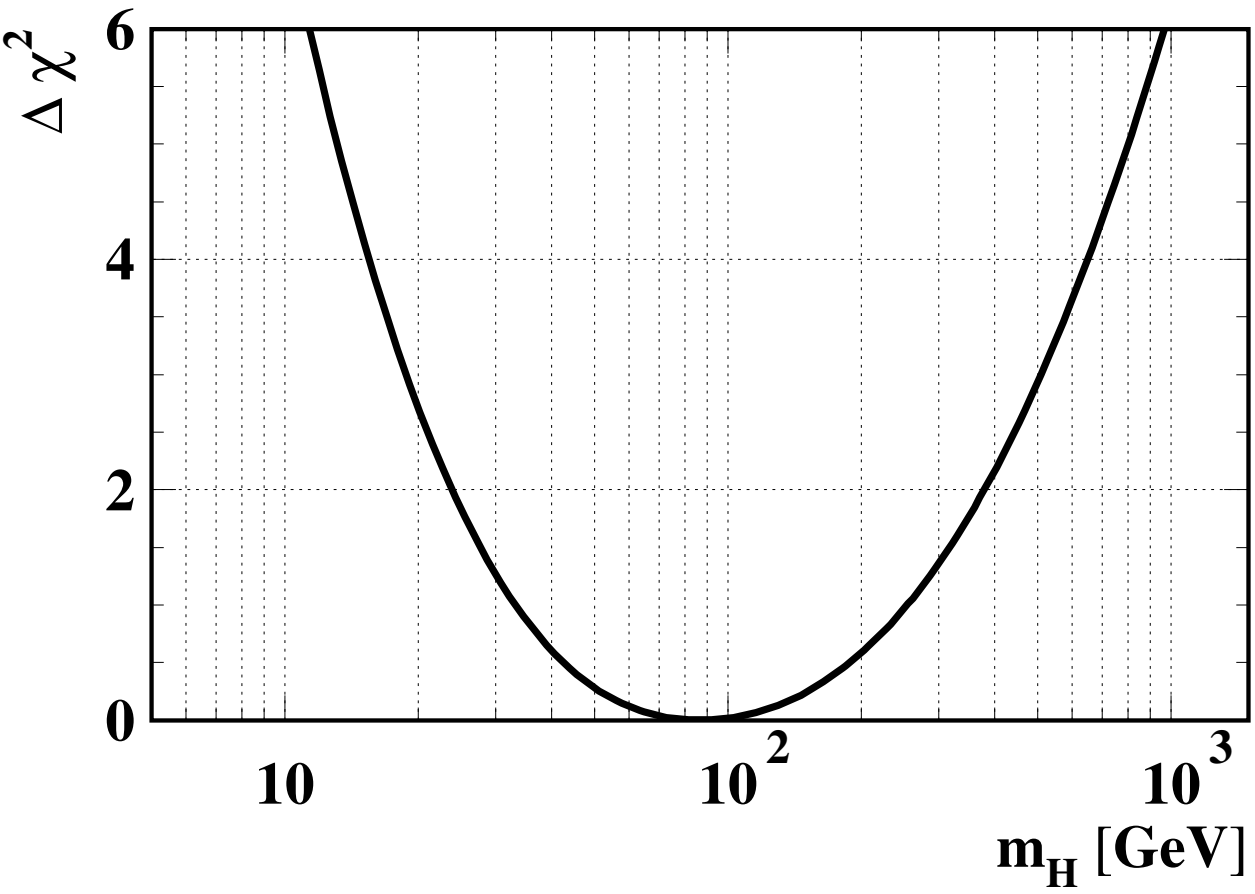

Figure 8: $\Delta\chi^2 = \chi^2 - \chi^2_{min}$ vs $m_{\rm H}$ for the data used for the fit in the last column of Table 20 and including the Tevatron value of $m_{\rm t}$.

Appendix

A The Measurements used in the Heavy Flavour Averages

Tagging	ALEPH 90-91 shape [45]	ALEPH 90-91 lepton [40]	ALEPH 92 lifetime [47]	DELPHI 90-93† multiple [48]	DELPHI 91-92 lepton [41]
R_b	0.2280	0.2162	0.2187	0.2210	0.2145
Statistical	0.0054	0.0062	0.0022	0.0016	0.0089
Uncorrelated	0.0036	0.0028	0.0022	0.0013	0.0063
Correlated	0.0032	0.0042	0.0012	0.0015	0.0023
Total Systematic	0.0048	0.0050	0.0025	0.0020	0.0067
a_c	-0.004		-0.014	-0.015	
R_c^{used}	0.165		0.171	0.171	

Tagging	L3 91 shape [46]	L3 90-91† lepton [43]	OPAL 92-94† multiple [49]	OPAL 90-91 lepton [44]	SLD 93-94 lepton [12]
R_b	0.2220	0.2187	0.2197	0.2250	0.2171
Statistical	0.0030	0.0081	0.0014	0.0110	0.0040
Uncorrelated	0.0053	0.0047	0.0012	0.0035	0.0027
Correlated	0.0036	0.0034	0.0018	0.0057	0.0026
Total Systematic	0.0064	0.0058	0.0022	0.0066	0.0037
a_c	-0.021	-0.023	-0.018	-0.013	-0.023
R_c^{used}	0.171	0.171	0.171	0.171	0.171
$a(BR(b \to \ell))$	-0.001				
$BR(b \to \ell)^{used}$	10.5				
$a(BR(bc\ell))$		0.034			
$BR(bc\ell)^{used}$		7.9			

Table 21: The measurements of R_b. Preliminary results are indicated by the symbol †. The correlated systematic entries are from sources shared with one or more other results in the table; the uncorrelated systematic entries are from the remaining sources. a_c denotes the dependence on the assumed R_c^{used}, which is also given. There is an additional +0.2 statistical and +0.2 systematic correlation between the first two ALEPH results [40, 45].

Tagging	ALEPH 90-91 lepton [40]	DELPHI 91-94† D [52]	DELPHI 91-92 lepton [41]	OPAL 90-94 multiple [53]
R_c	0.1670	0.1520	0.1625	0.1525
Statistical	0.0054	0.0070	0.0085	0.0061
Uncorrelated	0.0149	0.0095	0.0177	0.0084
Correlated	0.0114	0.0061	0.0111	0.0041
Total Systematic	0.0188	0.0113	0.0209	0.0093

Table 22: The measurements of R_c.

Tagging	ALEPH 90-93 lepton [40]	ALEPH 90-93 lepton [40]	ALEPH 90-93 lepton [40]	DELPHI 91-94† lepton [42]	DELPHI 91-94† $D^{*\pm}$ [42]	L3 90-93† lepton [43]	OPAL 91-94 jet [51]	OPAL 90-94† lepton [44]	OPAL 90-94† $D^{*\pm}$ [55]
$\sqrt{s}$ (GeV)	88.36	89.42	90.21	89.43	89.54	89.56	89.52	89.54	89.54
$A_{FB}^{b\bar{b}}(-2)$	-3.1	3.3	9.3	6.3	1.9	7.02	6.3	3.3	2.7
Statistical	11.0	3.0	5.8	3.8	10.5	3.50	3.4	3.0	6.9
Uncorrelated	0.0	0.0	0.0	0.2	1.1	0.35	0.2	0.7	3.8
Correlated	0.1	0.1	0.3	0.1	0.8	0.12	0.1	0.2	0.3
Total Systematic	0.1	0.1	0.3	0.2	1.4	0.37	0.2	0.8	3.8
$a(R_b)$				-0.007		-1.642	-1.8		
R_b^{used}				0.217		0.216	0.216		
$a(R_c)$				0.122		0.913	0.01	-0.658	
R_c^{used}				0.171		0.169	0.173	0.171	
$a(\overline{\chi})$				2.053					
$\overline{\chi}^{used}$				0.121					
$a(BR(b \to \ell))$				-0.971		-0.928			
$BR(b \to \ell)^{used}$				11.0		10.5			
$a(BR(bc\ell))$				0.158		-0.066			
$BR(bc\ell)^{used}$				7.9		7.9			
$a(A_{FB}^{c\bar{c}}(-2))$						-0.267	-0.205		
$A_{FB}^{c\bar{c}}(-2)^{used}$						-2.9	-3.16		

Table 23: The measurements of $A_{FB}^{b\bar{b}}(-2)$ (in units of 10^{-2}).

Tagging	ALEPH 90-93 lepton [40]	ALEPH 91-93 jet [50]	DELPHI 91-94† jet [42]	DELPHI 91-94† lepton [42]	DELPHI 91-94† $D^{*\pm}$ [42]	L3 90-93† lepton [43]	OPAL 91-94† jet [51]	OPAL 90-94† lepton [44]	OPAL 90-94† $D^{*\pm}$ [55]
$\sqrt{s}$ (GeV)	91.26	91.19	91.23	91.23	91.23	91.27	91.25	91.24	91.20
$A_{FB}^{b\bar{b}}(pk)$	8.43	9.92	9.90	10.49	7.1	10.3	9.73	10.30	11.2
Statistical	0.68	0.84	0.72	0.76	2.5	1.0	0.67	0.90	3.5
Uncorrelated	0.08	0.25	0.28	0.19	1.1	0.4	0.23	0.24	1.7
Correlated	0.11	0.28	0.25	0.24	0.8	0.1	0.32	0.27	1.0
Total Systematic	0.14	0.38	0.38	0.31	1.4	0.4	0.39	0.36	2.0
$a(R_b)$		-3.07	-0.6	-2.893		-1.642	-10.09		
R_b^{used}		0.2188	0.221	0.217		0.216	0.216		
$a(R_c)$		+2.57	0.24	1.221		0.913	0.109	1.71	
R_c^{used}		0.171	0.171	0.171		0.169	0.173	0.171	
$a(\overline{\chi})$				3.447					
$\overline{\chi}^{used}$				0.121					
$a(BR(b \to \ell))$				-3.559		-0.647			
$BR(b \to \ell)^{used}$				11.0		10.5			
$a(BR(bc\ell))$				0.474		-0.283			
$BR(bc\ell)^{used}$				7.9		7.9			
$a(A_{FB}^{c\bar{c}}(pk))$						0.580	0.457		
$A_{FB}^{c\bar{c}}(pk)^{used}$						6.3	6.1		

Table 24: The measurements of $A_{FB}^{b\bar{b}}(pk)$ (in units of 10^{-2}).

Tagging	ALEPH 90-93 lepton [40]	ALEPH 90-93 lepton [40]	ALEPH 90-93 lepton [40]	DELPHI 91-94† lepton [42]	DELPHI 91-94† $D^{*\pm}$ [42]	L3 90-93† lepton [43]	OPAL 91-94 jet [51]	OPAL 90-94† lepton [44]	OPAL 90-94† $D^{*\pm}$ [55]
$\sqrt{s}$ (GeV)	92.07	93.02	93.93	93.02	92.94	92.93	92.94	92.94	92.94
$A_{FB}^{b\bar{b}}(+2)$	5.1	10.5	11.8	14.9	5.6	11.0	17.3	12.1	-26.7
Statistical	4.9	2.4	7.5	3.6	9.6	2.9	2.9	2.7	14.0
Uncorrelated	0.0	0.0	0.0	0.5	1.1	0.4	0.6	0.6	4.0
Correlated	0.2	0.3	0.3	0.4	0.8	0.1	0.4	0.4	2.3
Total Systematic	0.2	0.3	0.3	0.6	1.4	0.4	0.7	0.7	4.6
$a(R_b)$				-2.893		-1.642	-18.32		
R_b^{used}				0.217		0.216	0.216		
$a(R_c)$				-0.977		0.913	0.157	2.631	
R_c^{used}				0.171		0.169	0.173	0.171	
$a(\overline{\chi})$				4.767					
$\overline{\chi}^{used}$				0.121					
$a(BR(b \to \ell))$				-3.235		-0.630			
$BR(b \to \ell)^{used}$				11.0		10.5			
$a(BR(bc\ell))$				0.474		-0.303			
$BR(bc\ell)^{used}$				7.9		7.9			
$a(A_{FB}^{c\bar{c}}(+2))$						1.113	0.840		
$A_{FB}^{c\bar{c}}(+2)^{used}$						12.1	12.0		

Table 25: The measurements of $A_{FB}^{b\bar{b}}(+2)$ (in units of 10^{-2}).

Tagging	ALEPH 91-94† $D^{*\pm}$ [54]	DELPHI 91-94† $D^{*\pm}$ [42]	OPAL 90-94† lepton [44]	OPAL 91-94† $D^{*\pm}$ [55]
$\sqrt{s}$ (GeV)	89.4	89.54	89.54	89.54
$A_{FB}^{c\bar{c}}(-2)$	-4.9	0.2	-21.1	-0.6
Statistical	7.6	5.2	4.8	6.8
Uncorrelated	0.8	0.6	2.9	1.2
Correlated	0.0	0.1	0.4	0.1
Total Systematic	0.8	0.6	2.9	1.2
$a(A_{FB}^{b\bar{b}}(-2))$	0.291			
$A_{FB}^{b\bar{b}}(-2)^{used}$	-1.7			
$a(R_c)$			11.97	
R_c^{used}			0.171	

Table 26: The measurements of $A_{FB}^{c\bar{c}}(-2)$ (in units of 10^{-2}).

Tagging	ALEPH 90-91 lepton [40]	ALEPH 91-94† $D^{*\pm}$ [54]	DELPHI 91-94† lepton [42]	DELPHI 91-94† $D^{*\pm}$ [42]	L3 90-93† lepton [43]	OPAL 90-94† lepton [44]	OPAL 90-94† $D^{*\pm}$ [55]
$\sqrt{s}$ (GeV)	91.26	91.2	91.23	91.23	91.24	91.24	91.20
$A_{FB}^{c\bar{c}}(pk)$	9.1	6.4	8.37	7.5	7.8	5.2	6.8
Statistical	2.0	1.3	1.39	1.2	3.7	1.0	1.4
Uncorrelated	1.5	0.2	0.91	0.6	2.4	0.8	0.7
Correlated	1.0	0.2	0.74	0.1	0.6	0.8	0.1
Total Systematic	1.9	0.3	1.18	0.6	2.5	1.2	0.7
$a(R_b)$			3.617		4.32		
R_b^{used}			0.217		0.216		
$a(R_c)$			-6.351		-6.76	-3.815	
R_c^{used}			0.171		0.169	0.171	
$a(BR(b \to \ell))$			4.853		3.501		
$BR(b \to \ell)^{used}$			11.0		10.5		
$a(BR(bc\ell))$			-3.792		-0.303		
$BR(bc\ell)^{used}$			7.9		7.9		
$a(A_{FB}^{b\bar{b}}(pk))$		-1.491			6.400		
$A_{FB}^{b\bar{b}}(pk)^{used}$		8.7			8.8		

Table 27: The measurements of $A_{FB}^{c\bar{c}}(pk)$ from D^* meson and lepton tag analyses (in units of 10^{-2}).

Tagging	ALEPH 91-94† $D^{*\pm}$ [54]	DELPHI 91-94† $D^{*\pm}$ [42]	OPAL 90-94† lepton [44]	OPAL 90-94† $D^{*\pm}$ [55]
$\sqrt{s}$ (GeV)	93.0	92.94	92.94	92.94
$A_{FB}^{c\bar{c}}(+2)$	10.9	8.0	9.0	17.1
Statistical	6.1	4.6	4.0	5.8
Uncorrelated	0.7	0.6	2.0	1.4
Correlated	0.3	0.1	0.2	0.1
Total Systematic	0.8	0.6	2.0	1.4
$a(A_{FB}^{b\bar{b}}(+2))$	-2.074			
$A_{FB}^{b\bar{b}}(+2)^{used}$	12.1			
$a(R_c)$			-4.735	
R_c^{used}			0.171	

Table 28: The measurements of $A_{FB}^{c\bar{c}}(+2)$ (in units of 10^{-2}).

Tagging	SLD 93-95† jet [15]	SLD 94-95† $K^{\pm}$ [16]	SLD 93-95† lepton [14]
$\sqrt{s}$ (GeV)	91.26	91.26	91.26
$\mathcal{A}_b$	0.843	0.907	0.865
Statistical	0.046	0.094	0.072
Uncorrelated	0.045	0.091	0.071
Correlated	0.020	0.013	0.017
Total Systematic	0.049	0.092	0.073
$a(R_b)$	-0.131	-0.022	-0.654
R_b^{used}	0.2180	0.2180	0.2180
$a(R_c)$	0.133	0.003	0.073
R_c^{used}	0.171	0.171	0.171
$a(\mathcal{A}_c)$	0.081	-0.133	
$\mathcal{A}_c^{used}$	0.666	0.666	
$a(\overline{\chi})$		0.223	0.020
$\overline{\chi}^{used}$		0.13	0.120
$a(BR(b \to \ell))$			-0.222
$BR(b \to \ell)^{used}$			10.8
$a(BR(bc\ell))$			0.064
$BR(bc\ell)^{used}$			9.3

Table 29: The measurements of $\mathcal{A}_b$.

Tagging	SLD 93-95† $D^{*\pm}$ [13]	SLD 93-95† lepton [14]
$\sqrt{s}$ (GeV)	91.26	91.26
$\mathcal{A}_c$	0.64	0.44
Statistical	0.11	0.11
Uncorrelated	0.05	0.08
Correlated	0.02	0.05
Total Systematic	0.06	0.10
$a(R_b)$		0.654
R_b^{used}		0.2180
$a(R_c)$		-0.452
R_c^{used}		0.171
$a(\mathcal{A}_b)$	-0.128	
$\mathcal{A}_b{}^{used}$	0.935	
$a(BR(b \to \ell))$		0.415
$BR(b \to \ell)^{used}$		10.8
$a(BR(bc\ell))$		-0.436
$BR(bc\ell)^{used}$		9.3

Table 30: The measurements of $\mathcal{A}_c$.

Tagging	ALEPH 90-91 lepton [40]	ALEPH 92-93† multiple [40]	DELPHI 91-92 lepton [41]	L3 90-91† lepton [43]	OPAL 90-91† lepton [44]
$BR(b \to \ell)(\%)$	11.20	11.01	11.21	11.44	10.50
Statistical	0.33	0.10	0.45	0.48	0.60
Uncorrelated	0.32	0.20	0.50	0.37	0.39
Correlated	0.27	0.21	0.48	0.22	0.54
Total Systematic	0.42	0.29	0.70	0.43	0.66
$a(R_c)$				0.611	0.224
R_c^{used}				0.171	0.171
$a(\overline{\chi})$		0.208			
$\overline{\chi}^{used}$		0.1261			
$a(BR(bc\ell))$				0.461	
$BR(bc\ell)^{used}$				7.9	

Table 31: The measurements of $BR(b \to \ell)$ from the lepton tag analyses.

Tagging	ALEPH 90-91 lepton [40]	ALEPH 92-93† multiple [40]	DELPHI 91-92 lepton [41]	OPAL 90-91† lepton [44]
BR(b $\rightarrow$ c $\rightarrow \ell^+$) (%)	8.81	7.68	7.70	8.30
Statistical	0.25	0.18	0.49	0.40
Uncorrelated	0.40	0.25	0.95	0.57
Correlated	0.69	0.42	0.83	0.39
Total Systematic	0.80	0.49	1.26	0.69
$a(R_c)$				0.316
R_c^{used}				0.171
$a(\overline{\chi})$		-0.511		
$\overline{\chi}^{used}$		0.1261		

Table 32: The measurements of BR(b $\rightarrow$ c $\rightarrow \ell^+$) from the lepton tag analyses.

Tagging	ALEPH 90-91 lepton [40]	DELPHI 91-92 lepton [41]	L3 90-93† lepton [43]	OPAL 90-91† lepton [44]
$\overline{\chi}$	0.0993	0.1500	0.1253	0.1440
Statistical	0.0073	0.0200	0.0110	0.0220
Uncorrelated	0.0028	0.0107	0.0053	0.0055
Correlated	0.0051	0.0119	0.0025	0.0028
Total Systematic	0.0058	0.0160	0.0058	0.0062
$a(R_b)$			0.001	
R_b^{used}			0.216	
$a(R_c)$			0.001	0.013
R_c^{used}			0.169	0.171
a(BR(b $\rightarrow \ell$))			0.046	
BR(b $\rightarrow \ell$)^{used}			10.5	
a(BR(bcℓ))			-0.0342	
BR(bcℓ)^{used}			7.9	

Table 33: The measurements of $\overline{\chi}$ from the lepton tag analyses.

References

[1] The LEP Collaborations ALEPH, DELPHI, L3, OPAL and the LEP Electroweak Working Group, *Combined Preliminary Data on* Z *Parameters from the LEP Experiments and Constraints on the Standard Model*, CERN-PPE/94-187.

[2] The working group on LEP energy, R. Assmann et al., Z. Phys. **C66** (1995) 567.

[3] S. Jadach, E. Richter-Wąs, B.F.L. Ward and Z. Wąs, *Higher-Order Radiative Corrections to Low-Angle Bhabha Scattering: The YFS Monte Carlo Approach*, CERN-TH/95-38, February 1995.

[4] M. L. Swartz, *Reevaluation of the Hadronic Contribution to* $\alpha(M_Z^2)$, SLAC-PUB-6710, November 1994.

[5] A.D. Martin and D. Zeppenfeld, Phys. Lett. **B345** (1994) 558.

[6] S. Eidelmann and F. Jegerlehner, *Hadronic contributions to* $(g-2)$ *of the leptons and to the effective fine structure constant* $\alpha(m_Z^2)$, PSI-PR-95-1, BUDKERINP 95-5, January 1995.

[7] H. Burkhardt and B. Pietrzyk, *Update of the hadronic contribution to the QED vacuum polarization*, LAPP–EXP–95.05, June 1995, to be published in Phys. Lett. B.

[8] CDF Collaboration, F. Abe *et al.*, Phys. Rev. Lett. **74** (1995) 2626.

[9] DØ Collaboration, S. Abachi *et al.*, Phys. Rev. Lett. **74** (1995) 2632.

[10] SLD Collaboration, K. Abe *et al.*, Phys. Rev. Lett **73** (1994) 25.

[11] SLD Collaboration, *Precision electroweak physics with the SLD/SLC the left-right polarization asymmetry.*, Contributed Paper to EPS-HEP-95 Brussels, **eps0654**;
C. Baltay, *Some Recent Results from SLC/SLD*, CERN Particle Physics Seminar, 12 June 1995.

[12] SLD Collaboration, *A Measurement of* R_b *using Lifetime Double Tag*, Contributed Paper to EPS-HEP-95 Brussels, **eps0222**.

[13] SLD Collaboration, *A Measurement of the Left-Right Forward-Backward Asymmetry for Charm Quarks with* D^{*+} *and* D^+ *Mesons* Contributed Paper to EPS-HEP-95 Brussels, **eps0248**.

[14] SLD Collaboration, *Measurement of* A_b *and* A_c *from the Left–Right Forward–Backward Asymmetry of Leptons in Hadronic Events at the* Z^0 *Resonance* Contributed Paper to EPS-HEP-95 Brussels, **eps0249**.

[15] SLD Collaboration, *Measurement of* A_b *at the* Z^0 *Resonance Using a Lifetime Tag and Momentum-Weighted Track Charge* Contributed Paper to EPS-HEP-95 Brussels, **eps0250**.

[16] SLD Collaboration, *Measurement of* A_b *at the* Z^0 *Resonance Using Identified Charged Kaons* Contributed Paper to EPS-HEP-95 Brussels, **eps0251**.

[17] CDHS Collaboration, H. Abramowicz *et al.*, Phys. Rev. Lett. **57** (1986) 298;
CDHS Collaboration, A. Blondel *et al.*, Z.Phys. **C45** (1990) 361.

[18] CHARM Collaboration, J.V. Allaby *et al.*, Phys. Lett. **B177** (1986) 446;
CHARM Collaboration, J.V. Allaby *et al.*, Z. Phys.**C36** (1987) 611.

[19] CCFR Collaboration, C.G. Arroyo *et al.*, Phys. Rev. Lett. **72** (1994) 3452;
CCFR Collaboration, *Precision Measurements of Electroweak Parameters from* νN *Scattering* , Contributed Paper to EPS-HEP-95 Brussels, **eps0041**.

[20] UA2 Collaboration, J. Alitti *et al.*, Phys. Lett. **B276** (1992) 354.

[21] CDF Collaboration, F. Abe *et al.*, Phys. Rev. Lett. **65** (1990) 2243 and Phys. Rev. **D43** (1991) 2070.

[22] CDF Collaboration, F. Abe *et al.*, *Measurement of the W Boson Mass*, FERMILAB-PUB-95/033-E and FERMILAB-PUB-95/035-1995.

[23] DØ Collaboration, preliminary result presented by C.K. Jung, *W Mass Measurements from DØ and CDF Experiments at the Tevatron*, talk given at the 27th ICHEP, Glasgow, Scotland, 20-27 July 1994.

[24] ALEPH Collaboration, D. Decamp *et al.*, Z. Phys. **C48** (1990) 365;
ALEPH Collaboration, D. Decamp *et al.*, Z. Phys. **C53** (1992) 1;
ALEPH Collaboration, D. Buskulic *et al.*, Z. Phys. **C60** (1993) 71;
ALEPH Collaboration, D. Buskulic *et al.*, Z. Phys. **C62** (1994) 539;
ALEPH Collaboration, *Preliminary Results on Z Production Cross-Section and Lepton Forward-Backward Asymmetries using the 1994 Data*, note ALEPH 95-084 PHYSIC 95-078, eps0398.

[25] DELPHI Collaboration, P. Aarnio *et al.*, Nucl. Phys. **B367** (1991) 511;
DELPHI Collaboration, P. Abreu *et al.*, Nucl. Phys. **B417** (1994) 3;
DELPHI Collaboration, P. Abreu *et al.*, Nucl. Phys. B**418** (1994) 403;
DELPHI Collaboration, DELPHI Note 95-62 PHYS 497, July 1995.

[26] L3 Collaboration, B. Adeva *et al.*, Z. Phys. **C51** (1991) 179;
L3 Collaboration, O. Adriani *et al.*, Phys. Rep. **236** (1993) 1;
L3 Collaboration, M. Acciarri *et al.*, Z. Phys. **C62** (1994) 551;
L3 Collaboration, L3 Electroweak Update for 1995 Brussels/Beijing, L3 Note 1809, July 14, 1995.

[27] OPAL Collaboration, G. Alexander *et al.*, Z. Phys. **C52** (1991) 175;
OPAL Collaboration, P.D. Acton *et al.*, Z. Phys. **C58** (1993) 219;
OPAL Collaboration, R. Akers *et al.*, Z. Phys. **C61** (1994) 19;
OPAL Collaboration, *A Preliminary Update of the* Z *Line Shape and Lepton Asymmetry Measurements with the 1993 and 1994 Data*, OPAL Internal Physics Note PN166, February 1995;
OPAL Collaboration, *The Preliminary OPAL SiW luminosity analysis: Results for the 1994 Summer conferences*, OPAL Internal Physics Note PN142, July 1994.

[28] M. Koratzinos private communication and minutes of the 64th meeting of the LEP energy calibration working group, 17 February 1995.

[29] The LEP Collaborations ALEPH, DELPHI, L3, OPAL and the LEP Electroweak Working Group, *Updated Parameters of the* Z *Resonance from Combined Preliminary Data of the LEP Experiments*, CERN-PPE/93-157.

[30] See, for example, M. Consoli *et al.*, in "Z Physics at LEP 1", CERN Report CERN 89-08 (1989), eds G. Altarelli, R. Kleiss and C. Verzegnassi, Vol. 1, p. 7.

[31] LEP Electroweak Working Group, *An Investigation of the Interference between Photon and Z-Boson Exchange*, Internal Note, LEPEWWG/LS/95-01, ALEPH 95-95 PHYSIC 95-87, DELPHI 95-138 PHYS 563, L3 Note 1812, OPAL Technical Note TN314, 1 August 1995.

[32] ALEPH Collaboration, D. Buskulic *et al.*, *Improved tau polarisation measurements*, CERN-PPE/95-023 (1995).

[33] DELPHI Collaboration, P. Abreu *et al.*, *Measurements of the τ Polarisation in Z^0 decays*, CERN–PPE/95–30 (1995).

[34] L3 Collaboration, O. Acciari *et al.*, Phys. Lett. **B341** (1994) 24;
L3 Collaboration, *A Prliminary Update of A_τ and A_e Using 1994 Data*, L3 Note 1793, July 5, 1995.

[35] OPAL Collaboration, *Updated Measurement of the Tau Polarisation Asymmetries*, OPAL Internal Physics Note PN172, March 1995.

[36] LEP Electroweak Working Group, *Combined LEP and SLD Electroweak Heavy Flavour Results for summer 1995 Conferences*, LEPHF/95-02, ALEPH Note 95-091 PHYSIC 95-084, DELPHI 95-115 PHYS 550, L3 Note 1813, OPAL Technical Note TN313, SLD Physics Note 39, 25 July 1995.

[37] LEP Electroweak Working Group, *A Consistent Treatment of Systematic Errors for LEP Electroweak Heavy Flavour Analyses*, LEPHF/94-01, ALEPH Note 94-30, DELPHI 94-23 Phys 357, L3 Note 1577, OPAL Technical Note TN213.

[38] LEP Electroweak Working Group, *Presentation of LEP Electroweak Heavy Flavour Analyses for Summer 1994 Conferences*, LEPHF/94-02, ALEPH Note 94-90, DELPHI 94-23/add, L3 Note 1613, OPAL Technical Note TN237.

[39] LEP Electroweak Working Group, *LEP Electroweak Heavy Flavour Results for Summer 1994 Conferences*, LEPHF/94-03, ALEPH Note 94-119 PHYSIC 94-103, DELPHI 94-108 PHYS 425, L3 Note 1630, OPAL Technical Note TN242.

[40] ALEPH Collaboration, D. Buskulic *et al.*, Z. Phys. **C62** (1994) 179;
ALEPH Collaboration, $B^0\overline{B^0}$ *mixing and* $b\overline{b}$ *asymmetry from high p_t leptons,* ALEPH 94-036, contributed paper to the La Thuile and Moriond Winter conferences, 1994;
ALEPH Collaboration, *Heavy Flavour Lepton Contribution for Summer 1994 Conferences,* ALEPH 94-123 PHYSIC 94-107;
ALEPH Collaboration., D. Buskulic *et al.*, *Measurement of the semileptonic b branching ratios from inclusive leptons in Z decays*, Contributed Paper to EPS-HEP-95 Brussels, **eps0404**.

[41] DELPHI Collab., P.Abreu et al., Z. Phys. **C66** (1995) 323.

[42] DELPHI Collaboration, P.Abreu *et al.*, Z.Phys **C65** (1995) 569;
DELPHI Collaboration, P.Abreu *et al.*, Z.Phys **C66** (1995) 341;
DELPHI Collaboration, *Measurement of the Forward-Backward Asymmetries of $e^+e^- \to Z \to b\overline{b}$ and $e^+e^- \to Z \to c\overline{c}$* Contributed Paper to EPS-HEP-95 Brussels, **eps0571**, DELPHI 95-87 PHYS 522.

[43] L3 Collaboration, O. Adriani *et al.*, Phys. Lett. **B292** (1992) 454;
L3 Collaboration, M. Acciarri *et al.*, Phys. Lett. **B335** (1994) 542;
L3 Collaboration, *Measurement of R_b and BR($b \to \ell X$) from b-quark semi-leptonic decays,* L3 internal note 1449, July 16 1993;
L3 Collaboration, *L3 Results on $A_{FB}^{b\bar{b}}$, $A_{FB}^{c\bar{c}}$ and χ for the Glasgow Conference,* L3 Note 1624;
L3 Collaboration, *L3 Results on R_b and* BR($b \to \ell$) *for the Glasgow Conference,* L3 Note 1625.
The sign of the uncertainties arising from the b semileptonic decay model have been corrected [56].

[44] OPAL Collaboration, R. Akers *et al.*, Z. Phys. **C60** (1993) 199;
OPAL Collaboration, *Measurement of the forward backward asymmetries of* $e^+e^- \to Z \to b\overline{b}$ *and* $e^+e^- \to Z \to c\overline{c}$ *from events tagged by a lepton, including 1994 data*, Contributed Paper to EPS-HEP-95 Brussels, **eps0279**.

[45] ALEPH Collaboration, D. Buskulic *et al.*, Phys. Lett. **B313** (1993) 549.

[46] L3 Collaboration, O. Adriani *et al.*, Phys. Lett. **B307** (1993) 237.

[47] ALEPH Collaboration, D. Buskulic *et al.*, Phys. Lett. **B313** (1993) 535.

[48] DELPHI Collaboration, *Measurement of the partial decay width* $R_b = \Gamma_{b\bar{b}}/\Gamma_{had}$ *with the DELPHI detector at LEP* , Contributed Paper to EPS-HEP-95 Brussels, **eps0570**.

[49] OPAL Collaboration, Z. Phys. **C65** (1995) 17-30;
An Update of the Measurement of $\Gamma_{\mathrm{b\bar{b}}}/\Gamma_{\mathrm{had}}$ *using a Double Tagging Method*, Contributed Paper to EPS-HEP-95 Brussels, **eps0278**, OPAL Physics Note PN181.

[50] ALEPH Collaboration, D. Buskulic *et al.*, Phys. Lett. **B335** (1994) 99.

[51] OPAL Collaboration, *A Measurement of the Forward-Backward asymmetry of* $\mathrm{e^+e^-} \to \mathrm{b\overline{b}}$ *applying a jet charge algorithm to lifetime tagged events,* CERN-PPE/95-50, Apr. 1995, submitted to Z. Phys. C.

[52] DELPHI Collaboration, *Study of Charm Mesons Production in* Z^0 *Decays and Measurement of* $\Gamma_{\mathrm{c}}/\Gamma_{\mathrm{h}}$ Contributed Paper to EPS-HEP-95 Brussels, **eps0557**, DELPHI 95-101 PHYS 536.

[53] OPAL Collaboration, R. Akers *et al..*, Z. Phys. C. **67** (1995) 27;
OPAL Collaboration, *A measurement of* $B(\mathrm{c} \to \mathrm{D}^\star)$ *and* $\Gamma_{c\bar{c}}/\Gamma_{had}$ *using a double tagging technique.*, Contributed Paper to EPS-HEP-95 Brussels, **eps0289**, OPAL physics note PN 175;
OPAL Collaboration, *A summary of OPAL measurements of charm production in* Z *decays.* OPAL Physics note PN190.

[54] ALEPH Collaboration, D. Buskulic *et al.*, Z. Phys. **C62** (1994) 1;
ALEPH Collaboration, D. Buskulic *et al.*, *The Forward–Backward Asymmetry for Charm Quarks at the Z pole : an Update*, Contributed Paper to EPS-HEP-95 Brussels, **eps0634**.

[55] OPAL Collaboration, *A Measurement of the Charm and Bottom Forward Backward Asymmetry using D Mesons with the OPAL Detector at LEP* Contributed Paper to EPS-HEP-95 Brussels, **eps0290**, OPAL Physics Note, PN183.

[56] LEP Electroweak Working Group, *LEP Electroweak Heavy Flavour Results for Winter 1995 Conferences*, LEPHF/95-01, ALEPH Note 95-037 PHYSIC 95-035, DELPHI 95-28 PHYS 479, L3 Note 1735, OPAL Technical Note TN283.

[57] D. Bardin *et al.*, Z. Phys. **C44** (1989) 493; Comp. Phys. Comm. **59** (1990) 303; Nucl. Phys. **B351**(1991) 1; Phys. Lett. **B255** (1991) 290 and CERN-TH 6443/92 (May 1992).

[58] A. Djouadi, B. Lampe and P.M. Zerwas, *A note on QCD corrections to Forward-Backward Asymmetries of Heavy-Quark Jets in Z Decays*, MPI-Ph/94-81.

[59] ALEPH Collaboration, D. Decamp *et al.*, Phys. Lett. **B259** (1991) 377.

[60] ALEPH Collaboration, ALEPH-Note 93-041 PHYSIC 93-032 (1993);
ALEPH Collaboration, ALEPH-Note 93-042 PHYSIC 93-034 (1993);
ALEPH Collaboration, ALEPH-Note 93-044 PHYSIC 93-036 (1993).

[61] ALEPH Collaboration, *Jet charge measurements in* $Z \to q\overline{q}$ *decays*, Contributed Paper to EPS-HEP-95 Brussels, **eps0449**.

[62] DELPHI Collaboration, P. Abreu *et al.*, Phys. Lett. **B277** (1992) 371.

[63] OPAL Collaboration, P. D. Acton *et al.*, Phys. Lett. **B294** (1992) 436.

[64] OPAL Collaboration, OPAL Physics Note PN195 (1995).

[65] CHARM II Collaboration, P. Vilain *et al.*, Phys. Lett. **B335** (1994) 246.

[66] S. Bethke, Proceedings of the QCD '94 conference, Montpellier, France, Nucl. Phys. B. (Proc. Suppl.) **39B,C** (1995) 198.

[67] The average for $m_{\rm W}$ has been performed taking into account the measurements [20–23]. The method of the combination follows the description in [72] treating the uncertainty due to parton distribution functions as the only common error. Measurements are averaged weighted by their uncorrelated uncertainties and then the largest parton distribution function uncertainty quoted, $\Delta m_{\rm W} = 0.085$ GeV [20], is included after averaging.

[68] Electroweak libraries:
ZFITTER: see Reference 57;
BHM: G. Burgers, W. Hollik and M. Martinez; M. Consoli, W. Hollik and F. Jegerlehner: Proceedings of the Workshop on Z physics at LEP I, CERN Report 89-08 Vol.I,7 and G. Burgers, F. Jegerlehner, B. Kniehl and J. Kühn: the same proceedings, CERN Report 89-08 Vol.I, 55.
These computer codes have recently been upgraded by including the results of [69] and references therein.

[69] *Reports of the working group on precision calculations for the Z resonance*, eds. D. Bardin, W. Hollik and G. Passarino, CERN Yellow Report 95-03, Geneva, 31 March 1995.

[70] A. Blondel and C. Verzegnassi, Phys. Lett. **B311** (1993) 346.

[71] T. Hebbeker, M. Martinez, G. Passarino and G. Quast, Phys. Lett. **B331** (1994) 165.

[72] M. Demarteau *et al.*, *Combining W Mass Measurements*, CDF/PHYS/CDF/PUBLIC/2552 and DØ NOTE 2115.